Journal of Sound and Vibration 329 (2010) 2241–2264

Contents lists available at ScienceDirect

Journal of Sound and Vibration

journal homepage: www.elsevier.com/locate/jsvi

Assessment of nanotube structures under a moving nanoparticle using nonlocal beam theories

Keivan Kiani [a,*], Bahman Mehri [b]

[a] Department of Civil Engineering, Sharif University of Technology, Azadi Ave., P.O. Box 11365-9313, Tehran, Iran
[b] Department of Mathematical Sciences, Sharif University of Technology, Tehran, Iran

ARTICLE INFO

Article history:
Received 23 June 2009
Received in revised form
10 December 2009
Accepted 13 December 2009
Handling Editor: H. Ouyang
Available online 12 January 2010

ABSTRACT

Dynamic analysis of nanotube structures under excitation of a moving nanoparticle is carried out using nonlocal continuum theory of Eringen. To this end, the nanotube structure is modeled by an equivalent continuum structure (ECS) according to the nonlocal Euler–Bernoulli, Timoshenko and higher order beam theories. The nondimensional equations of motion of the nonlocal beams acted upon by a moving nanoparticle are then established. Analytical solutions of the problem are presented for simply supported boundary conditions. The explicit expressions of the critical velocities of the nonlocal beams are derived. Furthermore, the capabilities of various nonlocal beam models in predicting the dynamic deflection of the ECS are examined through various numerical simulations. The role of the scale effect parameter, the slenderness ratio of the ECS and velocity of the moving nanoparticle on the time history of deflection as well as the dynamic amplitude factor of the nonlocal beams are scrutinized in some detail. The results show the importance of using nonlocal shear deformable beam theories, particularly for very stocky nanotube structures acted upon by a moving nanoparticle with low velocity.

1. Introduction

The capability of carbon nanotubes (CNTs) to interact with materials at the molecular scale along with their phenomenal electromechanical properties is introducing novel nanostructures with the task of nanoparticle transport [1–4]. The observation of Hummer et al. [1] showed that the CNTs could be exploited as unique molecular channels for water and protons. Recently, the traditional idea of making a molecular machine has been met in the real world of nanotechnology according to the literature [5–12]. These nanomachines are fueled by electrical voltage, chemical conversions, external light or temperature. For example, the molecular machine of Shirai et al. [9] is synthesized from four spherical molecules as wheels get their energy from temperature. They claimed to have observed the rotation of the spherical molecules such that each molecule moves along on its symmetry axis. The so-called nanocars or nanovehicles (i.e., moving nanoparticles) could move several nanometers in size depending on the temperature [9]. By being able to move molecules on a surface, the molecules can also be used as a transport vehicle of several atoms; therefore, it is often called as nanotruck [13]. In all these applications, one somehow faces the problem of nanostructure–moving nanoparticle interaction, mostly because of the mass weights of the nanoparticles and the friction between the surfaces of the nanoparticle and the nanotube structure.

* Corresponding author. Tel.: +98 21 6616 4264; fax: +98 21 6601 4828.
E-mail addresses: k_kiani@civil.sharif.edu, keivankiani@yahoo.com (K. Kiani), mehri@sharif.edu (B. Mehri).

0022-460X/$ - see front matter © 2010 Elsevier Ltd. All rights reserved.
doi:10.1016/j.jsv.2009.12.017

Conducting experimental tests at nanoscales are much harder than those at microscales. Moreover, molecular dynamics and quantum mechanics simulations involve huge computational efforts, especially for vibration of large-scale structures. To overcome these difficulties, suitable continuum beam models are successfully employed to study the overall behavior of the nanotube structures. In this regard, Gupta and Batra [14] proposed an equivalent continuum structure (ECS) whose frequencies in axial, torsional and radial breathing modes are equal to those of the single-walled carbon nanotubes (SWCNTs). It is found that the ECS made of a linear elastic homogeneous material is a cylindrical tube of mean radii and length equal to those of the SWCNT. The simulation results demonstrated that Young's modulus and shear modulus of the material of the ECS would be in turn 1 and 0.4 TPa for a wall thickness of the ECS equal to 3.4 Å.

On the other hand, new experimental results have explained the importance of size effect in the mechanical properties of material when the dimensions of the specimen become small [15]. The classical continuum theory (CCT) expresses that stress at each point of the medium would be independent of the stress at other points of the continua. Therefore, it is expected that CCT could not capture the real dynamic response of the continua, especially when the dimensions of the continua or the wavelength of the propagated sound wave would be comparable with the internal length scales of the continuum material. To conquer this weakness of the CCT, several modifications of the CCT have been proposed to admit size effect in the problem formulas. The gradient strains and integral nonlocal strains are two popular types of nonlocal continuum theories (NCTs) which include one or several internal length scales. Because of the aforementioned disadvantages of CCT, the application of the NCTs to various problems of nanostructures has been paid much attention by the nanotechnology communities of various disciplines. Peddieson et al. [16] applied the NCT to the Euler–Bernoulli beam (EB) to study the static response of nanoscale devices modeled as a cantilever and simply supported beam. In another work, the effect of the scale effect parameter on static deformation of micro- and nanostructures was investigated through nonlocal Euler–Bernoulli and Timoshenko beam theories by Wang and Liew [17]. The obtained results showed that the scale effect only takes effect for nanostructures of the size of nanometer; in other words, the beam models based on CCT would be satisfactory in static analysis and design of microdevices. Their investigation revealed that the shear effect could play an important role in static analyses of the nanostructures. In addition to the static analyses of the nanostructures, extensive research has been conducted for a better understanding of their mechanical behavior including column buckling assessment [18–21], resonant frequencies and mode shapes analyses [22–24], modeling sound wave propagation within the nanostructures [25–27], and vibration of tubular nanobeams coveying fluid [28–30]. As regards using different nonlocal beam theories for bending, buckling and free vibration problems, Reddy [31] reformulated the equations of motion of various beam theories, including the Euler–Bernoulli, Timoshenko, higher order, and Levinson beam models using the nonlocal constitutive relations of Eringen. The variational expressions in terms of displacements were also presented for various nonlocal beam models. Analytical solutions of bending, vibration and buckling were presented to show the effect of the nonlocality on static deflections, buckling loads and natural frequencies. A generalized nonlocal beam theory was proposed by Aydogdu [32] to examine bending, buckling and free vibration of nanobeams. Effects of nonlocality and length of beams were then investigated in some detail for each considered problem.

As it is seen, no detailed investigation on the dynamic effects of the moving nanoparticles on the nanotube structures is available in the literature at present. In this study, vibration of nanotube structures under a moving nanoparticle is examined by using the NCT of Eringen [33–35]. To this end, the nanotube structure is modeled by an EQS using nonlocal Euler–Bernoulli, Timoshenko and higher order beam theories. The obtained nonlocal equations of motion are solved analytically under simply supported conditions. The critical velocities of the moving nanoparticle associated with the nonlocal beam theories are introduced. The capabilities of the proposed nonlocal beam models in capturing the dynamic deflection of the nanotube structures are then examined through various numerical studies. Furthermore, the role of the scale effect parameter, the slenderness ratio of the nanostructure and velocity of the moving nanoparticle on the time history of deflections as well as the dynamic amplitude factor of the nanotube structures are studied in some detail.

2. Description and assumptions of the mathematical model

Consider an ECS associated with a nanotube structure subjected to a moving nanoparticle of mass weight mg and constant velocity v (see Fig. 1a). The ECS is restrained at both ends and axially fixed at one end (i.e., simply supported boundary conditions). The ECS is a homogeneous cylindrical tube of mean radii r_m and thickness t_b such that the inner and outer radii of the tube are $r_i = r_m - t_b/2$ and $r_o = r_m + t_b/2$, respectively (see Fig. 1 b). The following assumptions are made in the mathematical modeling of the problem: (1) The nanotube structure excited by a moving nanoparticle could be

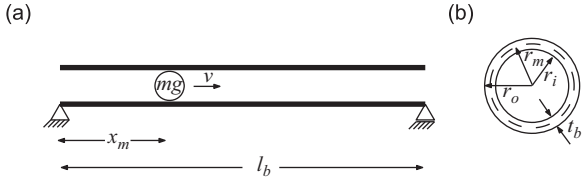

Fig. 1. (a) Schematic representation of an ECS model to study nanotube structures under excitation of a moving nanoparticle; (b) cross-section of the ECS.

modeled as an ECS under a moving point load. The vibration of the ECS is simulated by nanobeams based on the nonlocal Euler–Bernoulli beam theory (NEBT), nonlocal Timoshenko beam theory (NTBT), and nonlocal higher order beam theory (NHOBT). (2) The material of the ECS is linear isotropic homogeneous with Young's and shear modulus of E_b and G_b, correspondingly. (3) The cross-sectional area of the ECS, A_b, and the beam density, ρ_b, are uniform along its length. (4) At the time $t=0$, the moving nanoparticle enters the left end of the ECS. The only applied load on the ECS is due to the normal weight of the moving nanoparticle. Additionally, the moving nanoparticle would be in contact with the ECS during excitation and the inertial effects of the moving nanoparticle would be negligible, i.e., $mg(\mathrm{D}^2/\mathrm{D}t^2)w(x_m,t)=0$ where x_m is the position of the moving nanoparticle at each time (i.e., $x_m=v\,t$), $w(x,t)$ is the transverse displacement (deflection) of the nanobeam structure and $\mathrm{D}/\mathrm{D}t$ is the material derivative. (5) In application of the nonlocal continuum mechanics to the nanotube structures, the scale effect would be negligible across the thickness of the ECS.

3. Nonlocal continuum theory for beams

Based on the nonlocal continuum theory of Eringen [34,35], at an arbitrary point **x** of an elastic homogeneous isotropic continuum, the nonlocal stress tensor σ_{ij} is related to the local stress tensor t_{ij} by

$$[1-(e_0a)^2\nabla^2]\sigma_{ij}(\mathbf{x})=t_{ij}(\mathbf{x}), \tag{1}$$

where the parameter a denotes the internal characteristic length of the nanotube structure, ∇^2 is the Laplacian operator and e_0 is a constant associated with the material of the continuum. The value of e_0 is estimated such that the nonlocal continuum theory could successfully reproduce obtained dispersion curves by atomic models. A value of $e_0=0.39$ was suggested by Eringen [33]. By justification of the results of the higher order strain gradient for elastic beams with those of molecular dynamics, Wang and Hu [36] proposed $e_0=0.288$ for SWCNTs with armchair construction. Sudak [18] used $a=0.142$ nm for buckling analysis of multi-walled carbon nanotubes. In another study, Wang et al. [37] recommended a value of $e_0a=0.7$ nm for the application of the nonlocal elastic rod theory in prediction of axial stiffness of SWCNTs. The obtained results were compared with those of molecular dynamics and a good agreement was achieved. On the other hand, the nonlocal small scale parameter e_0a is commonly taken into account in the range of 0–2 nm [24,32,38] for the dynamic analyses of CNTs.

It is worth mentioning that one of the common concerns is about the accurate values of e_0a, used in nonlocal models for analyzing of nanostructures. A brief survey of the literature reveals that further research is still required to determine the realistic value of e_0a for each problem. Generally, this task could be carried out through justification of the results of the nonlocal elasticity theory with those of atomic-based models. In the present work, the effect of the nondimensional parameter e_0a/l_b (i.e., scale effect parameter) on the dynamic response of the nanotube structures under a moving nanoparticle is one of the objects to be investigated.

In an elastic homogeneous isotropic nanobeam, the only existing local stress fields are $t_{xx}=E_b\varepsilon_{xx}$ and $t_{xz}=G_b\gamma_{xz}$. Therefore, the only nonzero nonlocal stresses within the nanobeam structures are outlined as

$$\sigma_{xx}-(e_0a)^2\sigma_{xx,xx}=E_b\varepsilon_{xx},$$

$$\sigma_{xz}-(e_0a)^2\sigma_{xz,xx}=G_b\gamma_{xz}. \tag{2}$$

Hence, the nonlocal shear force ($Q_b=\int_{A_b}\sigma_{xz}\,\mathrm{d}A$), bending moment ($M_b=\int_{A_b}z\,\sigma_{xx}\,\mathrm{d}A$), and the third moment of the normal stress ($P_b=\int_{A_b}z^3\,\sigma_{xx}\,\mathrm{d}A$) or a combination of these stress resultants could be related to the local ones as

$$Q_b-(e_0a)^2Q_{b,xx}=Q_b^l,$$

$$M_b-(e_0a)^2M_{b,xx}=M_b^l,$$

$$(Q_b+\alpha P_{b,x})-(e_0a)^2(Q_b+\alpha P_{b,x})_{,xx}=Q_b^l+\alpha P_{b,x}^l, \tag{3}$$

where

$$Q_b^l=\int_{A_b}t_{xz}\,\mathrm{d}A,$$

$$M_b^l=\int_{A_b}z\,t_{xx}\,\mathrm{d}A,$$

$$P_b^l=\int_{A_b}z^3\,t_{xx}\,\mathrm{d}A, \tag{4}$$

in which the parameters associated with the local continuum theory are assigned with the superscript l.

4. Governing equations and analytical solutions of the problem based on various nonlocal beam theories

To obtain the governing equations based on the nonlocal continuum theory, it is required that the local stress resultants of the nanobeams in the equations of motion be replaced with those of the nonlocal ones for each beam theory such that Eq. (2) is satisfied. In the following subsections, the equations of motion of the nonlocal Euler–Bernoulli beam (NEB), nonlocal Timoshenko beam (NTB) and nonlocal higher order beam (NHOB) under excitation of a moving nanoparticle are obtained. Thereby, the analytical solutions of the governing equations are presented for simply supported beams using the Laplace transform method.

4.1. Application of the NEBT to nanotube structures subjected to a moving nanoparticle

4.1.1. Formulations of the NEB

The lateral equation of motion for a nanotube structure modeled as an Euler–Bernoulli beam, under a moving nanoparticle of weight mg and of velocity v based on classical continuum theory is given by [39]

$$\rho_b(A_b\ddot{w}^E - I_b\ddot{w}^E_{,xx}) - M^E_{b,xx} = mg\delta(x-x_m)H(l_b-x_m), \tag{5}$$

where δ and H are, respectively, the Dirac delta and Heaviside step functions, and $w^E(x,t)$ denotes the lateral displacement field associated with the EB. The local bending moment for an EB is defined as

$$(M^l_b)^E = -E_bI_bw^E_{,xx} \tag{6}$$

Substituting the equivalent value of $M^E_{b,xx}$ from Eq. (5) into Eq. (3) by using Eq. (6) leads to

$$M^E_b = -E_bI_bw^E_{,xx} + (e_0a)^2[\rho_b(A_b\ddot{w} - I_b\ddot{w}_{,xx}) - mg\delta(x-x_m)H(l_b-x_m)], \tag{7}$$

and by substituting M^E_b from Eq. (7) into Eq. (5), the nonlocal governing equation of the nanotube structure according to the NEBT could be derived as

$$\rho_bA_b[\ddot{w}^E - (e_0a)^2\ddot{w}^E_{,xx}] - \rho_bI_b[\ddot{w}^E_{,xx} - (e_0a)^2\ddot{w}^E_{,xxxx}] + E_bI_bw^E_{,xxxx} = mg[\delta(x-x_m) - (e_0a)^2\delta_{,xx}(x-x_m)]H(l_b-x_m). \tag{8}$$

Introducing dimensionless quantities for analyzing of not only a particular nanotube structure but also for a generalized one, regardless of the dimensions of the ECS

$$\xi = \frac{x}{l_b}, \quad \overline{w}^E = \frac{w^E}{l_b}, \quad \tau = \frac{1}{l_b^2}\sqrt{\frac{E_bI_b}{\rho_bA_b}}t, \quad \mu = \frac{e_0a}{l_b}, \quad \lambda = \frac{l_b}{r_b}, \quad \overline{f}^E = \frac{mgl_b^2}{E_bI_b}, \tag{9}$$

in which $r_b = \sqrt{I_b/A_b}$ represents the gyration radii of the cross-section of the ECS. Hence, the non-dimensional equation of motion becomes

$$\overline{w}^E_{,\tau\tau} - \mu^2\overline{w}^E_{,\tau\tau\xi\xi} - \frac{1}{\lambda^2}\overline{w}^E_{,\tau\tau\xi\xi} + \left(\frac{\mu}{\lambda}\right)^2\overline{w}^E_{,\tau\tau\xi\xi\xi\xi} + \overline{w}^E_{,\xi\xi\xi\xi} = \overline{f}^E[\delta(\xi-\xi_m) - \mu^2\delta_{,\xi\xi}(\xi-\xi_m)]H(1-\xi_m). \tag{10}$$

Furthermore, the nonlocal bending moment within the ECS based on NEBT at each phase could be calculated from the following equation:

$$M^E_b = \frac{E_bI_b}{l_b}\left[-\overline{w}^E_{,\xi\xi} + \mu^2\left(\overline{w}^E_{,\tau\tau} - \frac{1}{\lambda^2}\overline{w}^E_{,\tau\tau\xi\xi}\right)\right]. \tag{11}$$

4.1.2. Analytical solution of the governing equations of the NEB

Assumed mode method is employed to find the dynamic response of the nanotube structure modeled as an NEB. To this end, $\overline{w}^E(\xi,\tau) = \sum_{n=1}^{\infty}\phi^w_n(\xi)\,a^E_n(\tau)$ where $\phi^w_n(\xi) = \sin(n\pi\xi)$ is the n th mode shape associated with a simply supported NEB (see Appendix A.1). Moreover, $\delta(\xi-\xi_m) - \mu^2\delta_{,\xi\xi}(\xi-\xi_m) = \sum_{n=1}^{\infty}2(1+(n\pi\mu)^2)\sin(n\pi\xi_m)\sin(n\pi\xi)$. Therefore, one could readily arrive at the following ordinary differential equation (ODE) during the course of excitation

$$a^E_{n,\tau\tau} + \Gamma_n^2a^E_n = \beta^E_n\sin(g^E_n\tau), \tag{12}$$

with the initial conditions

$$a^E_n(0) = a^E_{n,\tau}(0) = 0, \tag{13}$$

where

$$\Gamma_n^2 = \frac{(n\pi)^4}{(1+(n\pi\mu)^2)\left(1+\left(\frac{n\pi}{\lambda}\right)^2\right)}, \quad \beta^E_n = \frac{2\overline{f}^E}{1+\left(\frac{n\pi}{\lambda}\right)^2}, \quad g^E_n = n\pi vl_b\sqrt{\frac{\rho_bA_b}{E_bI_b}}. \tag{14}$$

To solve Eq. (12) in time domain, Laplace transform is utilized. By recalling a property of this transform, $\mathcal{L}(a^E_{n,\tau\tau}) = s^2\mathcal{L}(a^E_n) - sa^E_n(0) - a^E_{n,\tau}(0)$, and applying Laplace transform to Eq. (12)

$$\mathcal{L}(a^E_n) = \frac{\beta^E_n g^E_n}{(s^2+(g^E_n)^2)(s^2+\Gamma^2_n)}. \tag{15}$$

Applying the inverse Laplace transform to Eq. (15), the dynamic deflection of the nanotube structure during the first phase of vibration is obtained as

$$\overline{w}^E(\xi,\tau) = \sum_{n=1}^{\infty} \frac{\beta^E_n}{\Gamma_n((g^E_n)^2-\Gamma^2_n)}[g^E_n \sin(\Gamma_n\tau) - \Gamma_n \sin(g^E_n\tau)]\sin(n\pi\xi). \tag{16}$$

To calculate the dynamic response during the course of free vibration (i.e., the second phase), the following ODE should be solved in the time domain

$$a^E_{n,\tau\tau} + \Gamma^2_n a^E_n = 0, \quad \tau > \tau^E_f \tag{17}$$

with the following initial conditions:

$$W^E_n = a^E_n(\tau^E_f) = \frac{\beta^E_n}{\Gamma_n((g^E_n)^2-\Gamma^2_n)}[g^E_n \sin(\Gamma_n\tau^E_f) - \Gamma_n \sin(g^E_n\tau^E_f)],$$

$$\dot{W}^E_n = a^E_{n,\tau}(\tau^E_f) = \frac{\beta^E_n g^E_n}{((g^E_n)^2-\Gamma^2_n)}[\cos(\Gamma_n\tau^E_f) - \cos(g^E_n\tau^E_f)]. \tag{18}$$

For the sake of simplicity, it is assumed that $\tau' = \tau - \tau^E_f$ where $\tau^E_f = 1/\nu l_b\sqrt{E_b I_b/\rho_b A_b}$. Solving the ODE of Eq. (17) via the Laplace transform method, the dynamic deflection of the NEB is readily derived during the second phase (i.e., $\tau' > 0$) as

$$\overline{w}^E(\xi,\tau) = \sum_{n=1}^{\infty}\left[W^E_n \cos(\Gamma_n\tau') + \frac{\dot{W}^E_n}{\Gamma_n}\sin(\Gamma_n\tau')\right]\sin(n\pi\xi). \tag{19}$$

4.2. Application of the NTBT to nanotube structures subjected to a moving nanoparticle

4.2.1. Formulations of the NTB

The equations of motion for a nanotube structure subjected to a moving nanoparticle, modeled as a Timoshenko beam, according to the CCT are expressed as [40]

$$\rho_b A_b \ddot{w}^{\mathrm{T}} - Q^{\mathrm{T}}_{b,x} = mg\delta(x-x_m)H(l_b-x_m),$$

$$\rho_b I_b \ddot{\theta}^{\mathrm{T}} - Q^{\mathrm{T}}_b + M^{\mathrm{T}}_{b,x} = 0, \tag{20}$$

where the local resultant shear force and bending moment associated with the Timoshenko beam are provided by

$$(Q^l_b)^{\mathrm{T}} = k_s G_b A_b (w^{\mathrm{T}}_{,x} - \theta^{\mathrm{T}}),$$

$$(M^l_b)^{\mathrm{T}} = -E_b I_b \theta^{\mathrm{T}}_{,x}, \tag{21}$$

in which θ denotes the angle of deflection and the parameter k_s is the shear correction factor which is a constant that depends on the cross-section geometry of the beam. By utilizing Eqs. (3) and (21), the nonlocal resultant shear force and bending moment of the NTB are obtained in terms of deformation fields and their derivatives as

$$Q^{\mathrm{T}}_b = k_s G_b A_b (w^{\mathrm{T}}_{,x} - \theta^{\mathrm{T}}) + (e_0 a)^2[\rho_b A_b \ddot{w}^{\mathrm{T}}_{,x} - mg\delta_{,x}(x-x_m)H(l_b-x_m)],$$

$$M^{\mathrm{T}}_b = -E_b I_b \theta^{\mathrm{T}}_{,x} + (e_0 a)^2[\rho_b A_b \ddot{w}^{\mathrm{T}} - \rho_b I_b \ddot{\theta}^{\mathrm{T}}_{,x} - mg\delta(x-x_m)H(l_b-x_m)]. \tag{22}$$

Therefore, by substituting Q^{T}_b and M^{T}_b from Eq. (22) into Eq. (20), the nonlocal governing equations of motion for an NTB could be obtained as

$$\rho_b A_b[\ddot{w}^{\mathrm{T}} - (e_0 a)^2 \ddot{w}^{\mathrm{T}}_{,xx}] - k_s G_b A_b (w^{\mathrm{T}}_{,xx} - \theta^{\mathrm{T}}_{,x}) = mg[\delta(x-x_m) - (e_0 a)^2 \delta_{,xx}(x-x_m)]H(l_b-x_m),$$

$$\rho_b I_b[\ddot{\theta}^{\mathrm{T}} - (e_0 a)^2 \ddot{\theta}^{\mathrm{T}}_{,xx}] - k_s G_b A_b (w^{\mathrm{T}}_{,x} - \theta^{\mathrm{T}}) - E_b I_b \theta^{\mathrm{T}}_{,xx} = 0. \tag{23}$$

The following dimensionless quantities are introduced for analyzing of the problem in a general form

$$\overline{w}^{\mathrm{T}} = \frac{w^{\mathrm{T}}}{l_b}, \quad \overline{\theta}^{\mathrm{T}} = \theta^{\mathrm{T}}, \quad \tau = \frac{1}{l_b}\sqrt{\frac{k_s G_b}{\rho_b}}t, \quad \eta = \frac{E_b I_b}{k_s G_b A_b l_b^2}, \quad \overline{f}^{\mathrm{T}} = \frac{mg}{k_s G_b A_b}. \tag{24}$$

Hence, the nonlocal nondimensional equations of motion of the nanotube structure based on the NTBT take the following form:

$$\overline{w}^{\mathrm{T}}_{,\tau\tau}-\mu^2\overline{w}^{\mathrm{T}}_{,\tau\tau\xi\xi}-\overline{w}^{\mathrm{T}}_{,\xi\xi}+\overline{\theta}^{\mathrm{T}}_{,\xi}=\overline{f}^{\mathrm{T}}[\delta(\xi-\xi_m)-\mu^2\delta_{,\xi\xi}(\xi-\xi_m)]H(1-\xi_m),$$

$$\frac{1}{\lambda^2}(\overline{\theta}^{\mathrm{T}}_{,\tau\tau}-\mu^2\overline{\theta}^{\mathrm{T}}_{,\tau\tau\xi\xi})-\overline{w}^{\mathrm{T}}_{,\xi}+\overline{\theta}^{\mathrm{T}}-\eta\overline{\theta}^{\mathrm{T}}_{,\xi\xi}=0. \tag{25}$$

Furthermore, the nonlocal bending moment within the NTB is obtained as follows from Eq. (22):

$$M^{\mathrm{T}}_b=k_sG_bA_bl_b\left\{-\eta\overline{\theta}^{\mathrm{T}}_{,\xi}+\mu^2\left[\overline{w}^{\mathrm{T}}_{,\tau\tau}-\frac{1}{\lambda^2}\overline{\theta}^{\mathrm{T}}_{,\tau\tau\xi}-\overline{f}^{\mathrm{T}}\delta(\xi-\xi_m)H(1-\xi_m)\right]\right\}. \tag{26}$$

4.2.2. Analytical solution of the governing equations of the NTB

The assumed mode method is utilized for discretization of the unknown fields of the problem in the spatial domain; therefore, $\overline{w}^{\mathrm{T}}(\xi,\tau)=\sum_{n=1}^{\infty}\phi^w_n(\xi)a^{\mathrm{T}}_n(\tau)$ and $\overline{\theta}^{\mathrm{T}}(\xi,\tau)=\sum_{n=1}^{\infty}\phi^\theta_n(\xi)b^{\mathrm{T}}_n(\tau)$ in which the parameters $\phi^w_n(\xi)$ and $\phi^\theta_n(\xi)$ denote in turn the appropriate n th mode shapes associated with the deflection and rotation fields of the nanotube structure modeled as an NTB. Moreover, $\phi^w_n(\xi)=\sin(n\pi\xi)$ and $\phi^\theta_n(\xi)=\cos(n\pi\xi)$ are derived as the mode shapes of a simply supported NTB (see Appendix A.2). Therefore, the following set of ODEs is obtained:

$$\begin{Bmatrix} a^{\mathrm{T}}_{n,\tau\tau} \\ b^{\mathrm{T}}_{n,\tau\tau} \end{Bmatrix}+\begin{bmatrix} \varsigma_{1_n} & \varsigma_{2_n} \\ \varsigma_{3_n} & \varsigma_{4_n} \end{bmatrix}\begin{Bmatrix} a^{\mathrm{T}}_n \\ b^{\mathrm{T}}_n \end{Bmatrix}=\begin{Bmatrix} \beta^{\mathrm{T}}_n\sin(g^{\mathrm{T}}_n\tau) \\ 0 \end{Bmatrix}, \tag{27}$$

with the initial conditions

$$\{a^{\mathrm{T}}_n(0),b^{\mathrm{T}}_n(0)\}^{\mathrm{T}}=\{a^{\mathrm{T}}_{n,\tau}(0),b^{\mathrm{T}}_{n,\tau}(0)\}^{\mathrm{T}}=\{0,0\}^{\mathrm{T}}, \tag{28}$$

where

$$\varsigma_{1_n}=\frac{(n\pi)^2}{1+(n\pi\mu)^2},\quad \varsigma_{2_n}=-\frac{n\pi}{1+(n\pi\mu)^2},$$

$$\varsigma_{3_n}=-\frac{n\pi\lambda^2}{1+(n\pi\mu)^2},\quad \varsigma_{4_n}=\frac{\lambda^2(1+\eta(n\pi)^2)}{1+(n\pi\mu)^2},$$

$$\beta^{\mathrm{T}}_n=2\overline{f}^{\mathrm{T}},\quad g^{\mathrm{T}}_n=n\pi\nu\sqrt{\frac{\rho_b}{k_sG_b}}. \tag{29}$$

The unknown parameters $a^{\mathrm{T}}_n(\tau)$ and $b^{\mathrm{T}}_n(\tau)$ of the ODEs set in Eq. (27) should be determined by a suitable method. To this end, Laplace transform is employed for solving Eq. (27) in the time domain. Hence, the Laplace transform of the unknown parameters are

$$\mathcal{L}(a^{\mathrm{T}}_n)=\frac{1}{\Delta^{\mathrm{T}}_n(s)}\frac{\beta^{\mathrm{T}}_ng^{\mathrm{T}}_n(s^2+\varsigma_{4_n})}{(s^2+(g^{\mathrm{T}}_n)^2)},$$

$$\mathcal{L}(b^{\mathrm{T}}_n)=-\frac{1}{\Delta^{\mathrm{T}}_n(s)}\frac{\beta^{\mathrm{T}}_ng^{\mathrm{T}}_n\varsigma_{3_n}}{(s^2+(g^{\mathrm{T}}_n)^2)}, \tag{30}$$

where

$$\Delta^{\mathrm{T}}_n(s)=(s^2+\varsigma_{1_n})(s^2+\varsigma_{4_n})-\varsigma_{2_n}\varsigma_{3_n}. \tag{31}$$

It can be readily shown that $\Delta^{\mathrm{T}}_n(s)=(s^2+(r^{\mathrm{T}}_{1_n})^2)(s^2+(r^{\mathrm{T}}_{2_n})^2)$ where

$$r^{\mathrm{T}}_{1_n}=\sqrt{(\varsigma_{1_n}+\varsigma_{4_n})/2-\sqrt{(\varsigma_{1_n}-\varsigma_{4_n})^2/4+\varsigma_{2_n}\varsigma_{3_n}}},$$

$$r^{\mathrm{T}}_{2_n}=\sqrt{(\varsigma_{1_n}+\varsigma_{4_n})/2+\sqrt{(\varsigma_{1_n}-\varsigma_{4_n})^2/4+\varsigma_{2_n}\varsigma_{3_n}}}. \tag{32}$$

Therefore, the dynamic deformation of the nanotube structure based on the NTBT is obtained as the following during the course of excitation:

$$\overline{w}^{\mathrm{T}}(\xi,\tau)=\sum_{n=1}^{\infty}\left[\frac{A^{\mathrm{T}}_{1_n}}{r^{\mathrm{T}}_{1_n}}\sin(r^{\mathrm{T}}_{1_n}\tau)+\frac{A^{\mathrm{T}}_{2_n}}{r^{\mathrm{T}}_{2_n}}\sin(r^{\mathrm{T}}_{2_n}\tau)+\frac{A^{\mathrm{T}}_{3_n}}{g^{\mathrm{T}}_n}\sin(g^{\mathrm{T}}_n\tau)\right]\sin(n\pi\xi),$$

$$\overline{\theta}^{\mathrm{T}}(\xi,\tau)=\sum_{n=1}^{\infty}\left[\frac{B_{1_n}^{\mathrm{T}}}{r_{1_n}^{\mathrm{T}}}\sin(r_{1_n}^{\mathrm{T}}\tau)+\frac{B_{2_n}^{\mathrm{T}}}{r_{2_n}^{\mathrm{T}}}\sin(r_{2_n}^{\mathrm{T}}\tau)+\frac{B_{3_n}^{\mathrm{T}}}{g_n^{\mathrm{T}}}\sin(g_n^{\mathrm{T}}\tau)\right]\cos(n\pi\xi), \tag{33}$$

where

$$A_{1_n}^{\mathrm{T}}=\frac{\beta_n^{\mathrm{T}}g_n^{\mathrm{T}}(\varsigma_{4_n}-(r_{1_n}^{\mathrm{T}})^2)}{((r_{2_n}^{\mathrm{T}})^2-(r_{1_n}^{\mathrm{T}})^2)((g_n^{\mathrm{T}})^2-(r_{1_n}^{\mathrm{T}})^2)},\quad B_{1_n}^{\mathrm{T}}=-\frac{\beta_n^{\mathrm{T}}g_n^{\mathrm{T}}\varsigma_{3_n}}{((r_{2_n}^{\mathrm{T}})^2-(r_{1_n}^{\mathrm{T}})^2)((g_n^{\mathrm{T}})^2-(r_{1_n}^{\mathrm{T}})^2)},$$

$$A_{2_n}^{\mathrm{T}}=-\frac{\beta_n^{\mathrm{T}}g_n^{\mathrm{T}}(\varsigma_{4_n}-(r_{2_n}^{\mathrm{T}})^2)}{((r_{2_n}^{\mathrm{T}})^2-(r_{1_n}^{\mathrm{T}})^2)((g_n^{\mathrm{T}})^2-(r_{2_n}^{\mathrm{T}})^2)},\quad B_{2_n}^{\mathrm{T}}=\frac{\beta_n^{\mathrm{T}}g_n^{\mathrm{T}}\varsigma_{3_n}}{((r_{2_n}^{\mathrm{T}})^2-(r_{1_n}^{\mathrm{T}})^2)((g_n^{\mathrm{T}})^2-(r_{2_n}^{\mathrm{T}})^2)},$$

$$A_{3_n}^{\mathrm{T}}=\frac{\beta_n^{\mathrm{T}}g_n^{\mathrm{T}}(\varsigma_{4_n}-(g_n^{\mathrm{T}})^2)}{((r_{1_n}^{\mathrm{T}})^2-(g_n^{\mathrm{T}})^2)((r_{2_n}^{\mathrm{T}})^2-(g_n^{\mathrm{T}})^2)},\quad B_{3_n}^{\mathrm{T}}=-\frac{\beta_n^{\mathrm{T}}g_n^{\mathrm{T}}\varsigma_{3_n}}{((r_{1_n}^{\mathrm{T}})^2-(g_n^{\mathrm{T}})^2)((r_{2_n}^{\mathrm{T}})^2-(g_n^{\mathrm{T}})^2)}. \tag{34}$$

The governing equations of the NTB during the course of free vibration can be obtained from Eq. (27) by setting $\beta_n^{\mathrm{T}}=0$

$$\begin{Bmatrix}a_{n,\tau\tau}^{\mathrm{T}}\\ b_{n,\tau\tau}^{\mathrm{T}}\end{Bmatrix}+\begin{bmatrix}\varsigma_{1_n} & \varsigma_{2_n}\\ \varsigma_{3_n} & \varsigma_{4_n}\end{bmatrix}\begin{Bmatrix}a_n^{\mathrm{T}}\\ b_n^{\mathrm{T}}\end{Bmatrix}=\begin{Bmatrix}0\\ 0\end{Bmatrix},\quad \tau>\tau_f^{\mathrm{T}} \tag{35}$$

and the initial conditions associated with the n th modes of vibration are

$$a_n^{\mathrm{T}}(\tau_f^{\mathrm{T}})=W_n^{\mathrm{T}}=\frac{A_{1_n}^{\mathrm{T}}}{r_{1_n}^{\mathrm{T}}}\sin(r_{1_n}^{\mathrm{T}}\tau_f^{\mathrm{T}})+\frac{A_{2_n}^{\mathrm{T}}}{r_{2_n}^{\mathrm{T}}}\sin(r_{2_n}^{\mathrm{T}}\tau_f^{\mathrm{T}})+\frac{A_{3_n}^{\mathrm{T}}}{g_n^{\mathrm{T}}}\sin(g_n^{\mathrm{T}}\tau_f^{\mathrm{T}}),$$

$$b_n^{\mathrm{T}}(\tau_f^{\mathrm{T}})=\Theta_n^{\mathrm{T}}=\frac{B_{1_n}^{\mathrm{T}}}{r_{1_n}^{\mathrm{T}}}\sin(r_{1_n}^{\mathrm{T}}\tau_f^{\mathrm{T}})+\frac{B_{2_n}^{\mathrm{T}}}{r_{2_n}^{\mathrm{T}}}\sin(r_{2_n}^{\mathrm{T}}\tau_f^{\mathrm{T}})+\frac{B_{3_n}^{\mathrm{T}}}{g_n^{\mathrm{T}}}\sin(g_n^{\mathrm{T}}\tau_f^{\mathrm{T}}), \tag{36}$$

and

$$a_{n,\tau}^{\mathrm{T}}(\tau_f^{\mathrm{T}})=\dot{W}_n^{\mathrm{T}}=A_{1_n}^{\mathrm{T}}\cos(r_{1_n}^{\mathrm{T}}\tau_f^{\mathrm{T}})+A_{2_n}^{\mathrm{T}}\cos(r_{2_n}^{\mathrm{T}}\tau_f^{\mathrm{T}})+A_{3_n}^{\mathrm{T}}\cos(g_n^{\mathrm{T}}\tau_f^{\mathrm{T}}),$$

$$b_{n,\tau}^{\mathrm{T}}(\tau_f^{\mathrm{T}})=\dot{\Theta}_n^{\mathrm{T}}=B_{1_n}^{\mathrm{T}}\cos(r_{1_n}^{\mathrm{T}}\tau_f^{\mathrm{T}})+B_{2_n}^{\mathrm{T}}\cos(r_{2_n}^{\mathrm{T}}\tau_f^{\mathrm{T}})+B_{3_n}^{\mathrm{T}}\cos(g_n^{\mathrm{T}}\tau_f^{\mathrm{T}}), \tag{37}$$

in which $\tau_f^{\mathrm{T}}=(1/v)\sqrt{k_sG_b/\rho_b}$. By taking Laplace transform of Eq. (35) with the initial conditions in Eqs. (36) and (37), one may write

$$\mathcal{L}(a_n^{\mathrm{T}})=\frac{(sW_n^{\mathrm{T}}+\dot{W}_n^{\mathrm{T}})(s^2+\varsigma_{4_n})-\varsigma_{2_n}(s\Theta_n^{\mathrm{T}}+\dot{\Theta}_n^{\mathrm{T}})}{(s^2+(r_{1_n}^{\mathrm{T}})^2)(s^2+(r_{2_n}^{\mathrm{T}})^2)},$$

$$\mathcal{L}(b_n^{\mathrm{T}})=\frac{(s\Theta_n^{\mathrm{T}}+\dot{\Theta}_n^{\mathrm{T}})(s^2+\varsigma_{1_n})-\varsigma_{3_n}(sW_n^{\mathrm{T}}+\dot{W}_n^{\mathrm{T}})}{(s^2+(r_{1_n}^{\mathrm{T}})^2)(s^2+(r_{2_n}^{\mathrm{T}})^2)}, \tag{38}$$

and the dynamic response of the system during the course of free vibration could be derived as the following:

$$\overline{w}^{\mathrm{T}}(\xi,\tau)=\sum_{n=1}^{\infty}\left[\frac{A_{1_n}^{'T}}{r_{1_n}^{\mathrm{T}}}\sin(r_{1_n}^{\mathrm{T}}\tau')+\frac{A_{2_n}^{'T}}{r_{2_n}^{\mathrm{T}}}\sin(r_{2_n}^{\mathrm{T}}\tau')+A_{3_n}^{'T}\cos(r_{1_n}^{\mathrm{T}}\tau')+A_{4_n}^{'T}\cos(r_{2_n}^{\mathrm{T}}\tau')\right]\sin(n\pi\xi),$$

$$\overline{\theta}^{\mathrm{T}}(\xi,\tau)=\sum_{n=1}^{\infty}\left[\frac{B_{1_n}^{'T}}{r_{1_n}^{\mathrm{T}}}\sin(r_{1_n}^{\mathrm{T}}\tau')+\frac{B_{2_n}^{'T}}{r_{2_n}^{\mathrm{T}}}\sin(r_{2_n}^{\mathrm{T}}\tau')+B_{3_n}^{'T}\cos(r_{1_n}^{\mathrm{T}}\tau')+B_{4_n}^{'T}\cos(r_{2_n}^{\mathrm{T}}\tau')\right]\cos(n\pi\xi), \tag{39}$$

where

$$\tau'=\tau-\tau_f^{\mathrm{T}},$$

$$A_{1_n}^{'T}=[(\dot{W}_n^{\mathrm{T}}\varsigma_{4_n}-\dot{W}_n^{\mathrm{T}}\varsigma_{2_n})-\dot{W}_n^{\mathrm{T}}(r_{1_n}^{\mathrm{T}})^2]/((r_{2_n}^{\mathrm{T}})^2-(r_{1_n}^{\mathrm{T}})^2),$$

$$B_{1_n}^{'T}=[(\dot{\Theta}_n^{\mathrm{T}}\varsigma_{1_n}-\dot{W}_n^{\mathrm{T}}\varsigma_{3_n})-\dot{\Theta}_n^{\mathrm{T}}(r_{1_n}^{\mathrm{T}})^2]/((r_{2_n}^{\mathrm{T}})^2-(r_{1_n}^{\mathrm{T}})^2),$$

$$A_{2_n}^{'T}=-[(\dot{W}_n^{\mathrm{T}}\varsigma_{4_n}-\dot{W}_n^{\mathrm{T}}\varsigma_{2_n})-\dot{W}_n^{\mathrm{T}}(r_{2n}^{\mathrm{T}})^2]/((r_{2_n}^{\mathrm{T}})^2-(r_{1_n}^{\mathrm{T}})^2),$$

$$B_{2_n}^{'T}=-[(\dot{\Theta}_n^{\mathrm{T}}\varsigma_{1_n}-\dot{W}_n^{\mathrm{T}}\varsigma_{3_n})-\dot{\Theta}_n^{\mathrm{T}}(r_{2_n}^{\mathrm{T}})^2]/((r_{2_n}^{\mathrm{T}})^2-(r_{1_n}^{\mathrm{T}})^2),$$

$$A_{3_n}^{'T}=[(W_n^{\mathrm{T}}\varsigma_{4_n}-W_n^{\mathrm{T}}\varsigma_{2_n})-W_n^{\mathrm{T}}(r_{1_n}^{\mathrm{T}})^2]/((r_{2_n}^{\mathrm{T}})^2-(r_{1_n}^{\mathrm{T}})^2),$$

$$B'^{T}_{3_n}=[(\Theta^{T}_{n}\varsigma_{1_n}-W^{T}_{n}\varsigma_{3_n})-W^{T}_{n}(r^{T}_{1_n})^2]/((r^{T}_{2_n})^2-(r^{T}_{1_n})^2),$$

$$A'^{T}_{4_n}=-[(W^{T}_{n}\varsigma_{4_n}-W^{T}_{n}\varsigma_{2_n})-W^{T}_{n}(r^{T}_{2_n})^2]/((r^{T}_{2_n})^2-(r^{T}_{1_n})^2),$$

$$B'^{T}_{4_n}=-[(\Theta^{T}_{n}\varsigma_{1_n}-W^{T}_{n}\varsigma_{3_n})-\Theta^{T}_{n}(r^{T}_{2_n})^2]/((r^{T}_{2_n})^2-(r^{T}_{1_n})^2). \tag{40}$$

4.3. Application of the NHOBT to nanotube structures subjected to a moving nanoparticle

4.3.1. Formulations of the NHOB

The local equations of motion for a nanotube structure excited by a moving nanoparticle model based on higher order beam theory are expressed as [41]

$$I_0\ddot{w}^H-(\alpha^2I_6-\alpha I_4)\ddot{\psi}^H_{,x}-\alpha^2I_6\ddot{w}^H_{,xx}-Q^H_{b,x}-\alpha P^H_{b,xx}=mg\delta(x-x_m)H(l_b-x_m),$$

$$(I_2-2\alpha I_4+\alpha^2I_6)\ddot{\psi}^H+(\alpha^2I_6-\alpha I_4)\ddot{w}^H_{,x}+Q^H_b+\alpha P^H_{b,x}-M^H_{b,x}=0, \tag{41}$$

where the local versions of Q^H_b, P^H_b and M^H_b are

$$(Q^l_b)^H=\kappa(\psi^H+w^H_{,x}),$$

$$(P^l_b)^H=J_4\psi^H_{,x}-\alpha J_6(\psi^H_{,x}+w^H_{,xx}),$$

$$(M^l_b)^H=J_2\psi^H_{,x}-\alpha J_4(\psi^H_{,x}+w^H_{,xx}), \tag{42}$$

in which

$$\kappa=\int_{A_b}G_b(1-3\alpha z^2)\,dA,$$

$$I_n=\int_{A_b}\rho_b z^n\,dA,\quad n=0,2,4,6,$$

$$J_n=\int_{A_b}E_b z^n\,dA,\quad n=2,4,6. \tag{43}$$

The value of the parameter α is determined such that the shear stress vanishes at the outer surfaces of the nanotube structure. Recalling $M^H_b-(e_0a)^2M^H_{b,xx}=J_2\psi^H_{,x}-\alpha J_4(\psi^H_{,x}+w^H_{,xx})$ and $(Q_b+\alpha P_{b,x})^H-(e_0a)^2(Q_b+\alpha P_{b,x})^H_{,xx}=\kappa(\psi^H+w^H_{,x})+(\alpha J_4-\alpha^2J_6)\psi^H_{,xx}-\alpha^2J_6w^H_{,xxx}$, and using the local equations of motion

$$M^H_b=J_2\psi^H_{,x}-\alpha J_4(\psi^H_{,x}+w^H_{,xx})+(e_0a)^2[(I_2-\alpha I_4)\ddot{\psi}^H_{,x}+I_0\ddot{w}^H-\alpha I_4\ddot{w}^H_{,xx}-mg\delta(x-x_m)H(l_b-x_m)],$$

$$Q^H_b+\alpha P^H_{b,x}=\kappa(\psi^H+w^H_{,x})+(\alpha J_4-\alpha^2J_6)\psi^H_{,xx}-\alpha^2J_6w^H_{,xxx}+(e_0a)^2[I_0\ddot{w}^H_{,x}+(\alpha I_4-\alpha^2I_6)\ddot{\psi}^H_{,xx}-\alpha^2I_6\ddot{w}^H_{,xxx}-mg\delta_{,x}(x-x_m)H(l_b-x_m)]. \tag{44}$$

By substituting M^H_b and Q^H_b from Eq. (44) into Eq. (41), the nonlocal governing equations of a nanotube structure based on HOBT are derived as

$$I_0[\ddot{w}^H-(e_0a)^2\ddot{w}^H_{,xx}]-(\alpha^2I_6-\alpha I_4)[\ddot{\psi}^H_{,x}-(e_0a)^2\ddot{\psi}^H_{,xxx}]-\alpha^2I_6[\ddot{w}^H_{,xx}-(e_0a)^2\ddot{w}^H_{,xxxx}]-\kappa(\psi^H_{,x}+w^H_{,xx})+(\alpha^2J_6-\alpha J_4)\psi^H_{,xxx}+\alpha^2J_6w^H_{,xxxx}$$
$$=mg[\delta(x-x_m)-(e_0a)^2\delta_{,xx}(x-x_m)]H(l_b-x_m),$$

$$(I_2-2\alpha I_4+\alpha^2I_6)[\ddot{\psi}^H-(e_0a)^2\ddot{\psi}^H_{,xx}]+(\alpha^2I_6-\alpha I_4)[\ddot{w}^H_{,x}-(e_0a)^2\ddot{w}^H_{,xxx}]-(J_2-2\alpha J_4+\alpha^2J_6)\psi^H_{,xx}-(\alpha^2J_6-\alpha J_4)w^H_{,xxx}=0. \tag{45}$$

To generalize, the governing equations of the problem may be expressed in dimensionless terms by defining the following nondimensional quantities:

$$\overline{w}^H=\frac{w^H}{l_b},\quad \overline{\psi}^H=\psi^H,\quad \tau=\frac{\alpha}{l_b^2}\sqrt{\frac{J_6}{I_0}}t,\quad \overline{f}^H=\frac{mgl_b^2}{\alpha^2J_6}, \tag{46}$$

substituting these terms into Eq. (45) leads to the nonlocal equations of motion in dimensionless form as follows:

$$\overline{w}^H_{,\tau\tau}-\mu^2\overline{w}^H_{,\tau\tau\xi\xi}+\gamma_1^2(\overline{\psi}^H_{,\tau\tau\xi}-\mu^2\overline{\psi}^H_{,\tau\tau\xi\xi\xi})-\gamma_2^2(\overline{w}^H_{,\tau\tau\xi\xi}-\mu^2\overline{w}^H_{,\tau\tau\xi\xi\xi\xi})-\gamma_3^2(\overline{\psi}^H_{,\xi}+\overline{w}^H_{,\xi\xi})-\gamma_4^2\overline{\psi}^H_{,\xi\xi\xi}+\overline{w}^H_{,\xi\xi\xi\xi}=\overline{f}^H[\delta(\xi-\xi_m)-\mu^2\delta_{,\xi\xi}(\xi-\xi_m)]H(1-\xi_m),$$

$$\overline{\psi}^H_{,\tau\tau}-\mu^2\overline{\psi}^H_{,\tau\tau\xi\xi}-\gamma_6^2(\overline{w}^H_{,\tau\tau\xi}-\mu^2\overline{w}^H_{,\tau\tau\xi\xi\xi})+\gamma_7^2(\overline{\psi}^H+\overline{w}^H_{,\xi})-\gamma_8^2\overline{\psi}^H_{,\xi\xi}+\gamma_9^2\overline{w}^H_{,\xi\xi\xi}=0, \tag{47}$$

where

$$\gamma_1^2=\frac{\alpha I_4-\alpha^2 I_6}{I_0 l_b^2},\quad \gamma_2^2=\frac{\alpha^2 I_6}{I_0 l_b^2},\quad \gamma_3^2=\frac{\kappa l_b^2}{\alpha^2 J_6},\quad \gamma_4^2=\frac{\alpha J_4-\alpha^2 J_6}{\alpha^2 J_6},\quad \gamma_6^2=\frac{\alpha I_4-\alpha^2 I_6}{I_2-2\alpha I_6+\alpha^2 I_6},$$

$$\gamma_7^2=\frac{\kappa I_0 l_b^4}{(I_2-2\alpha I_4+\alpha^2 I_6)\alpha^2 J_6},\quad \gamma_8^2=\frac{(J_2-2\alpha J_4+\alpha^2 J_6)I_0 l_b^2}{(I_2-2\alpha I_4+\alpha^2 I_6)\alpha^2 J_6},\quad \gamma_9^2=\frac{(\alpha J_4-\alpha^2 J_6)I_0 l_b^2}{(I_2-2\alpha I_4+\alpha^2 I_6)\alpha^2 J_6}. \tag{48}$$

Moreover, the nonlocal bending moment in the nanotube structure modeled based on the NHOBT is rewritten as

$$M_b^H=\frac{J_2}{l_b}\overline{\psi}^H_{,\xi}-\frac{\alpha J_4}{l_b}(\overline{\psi}^H_{,\xi}+\overline{w}^H_{,\xi\xi})+\mu^2\left[\frac{(I_2-\alpha I_4)\alpha^2 J_6}{I_0 l_b^3}\overline{\psi}^H_{,\xi\tau\tau}+\frac{\alpha^2 J_6}{l_b}\overline{w}^H_{,\tau\tau}-\frac{\alpha^3 I_4 J_6}{I_0 l_b^3}\overline{w}^H_{,\tau\tau\xi\xi}-mgl_b\delta(\xi-\xi_m)H(1-\xi_m)\right], \tag{49}$$

4.3.2. Analytical solution of the governing equations of the NHOB

The assumed mode method is employed for discretization of the unknown fields of the NHOB in the spatial domain; therefore, $\overline{w}^H(\xi,\tau)=\sum_{n=1}^{\infty}\phi_n^w(\xi)a_n^H(\tau)$ and $\overline{\psi}^H(\xi,\tau)=\sum_{n=1}^{\infty}\phi_n^\psi(\xi)b_n^H(\tau)$ in which the parameters $\phi_n^w(\xi)$ and $\phi_n^\psi(\xi)$ represent the n th mode shapes associated with the deflection and rotation of the NHOB, correspondingly. For an NHOB with simply supported boundary conditions, it can be shown that $\phi_n^w(\xi)=\sin(n\pi\xi)$ and $\phi_n^\psi(\xi)=\cos(n\pi\xi)$ (see Appendix A.3). Therefore, one could arrive at

$$\begin{bmatrix}\zeta_{1_n} & \zeta_{2_n}\\ \zeta_{3_n} & \zeta_{4_n}\end{bmatrix}\begin{Bmatrix}a^H_{n,\tau\tau}\\ b^H_{n,\tau\tau}\end{Bmatrix}+\begin{bmatrix}\eta_{1_n} & \eta_{2_n}\\ \eta_{3_n} & \eta_{4_n}\end{bmatrix}\begin{Bmatrix}a^H_n\\ b^H_n\end{Bmatrix}=\begin{Bmatrix}\beta_n^H\sin(g_n^H\tau)\\ 0\end{Bmatrix}, \tag{50}$$

with the following initial conditions:

$$\{a_n^H(0),b_n^H(0)\}^{\mathrm{T}}=\{a^H_{n,\tau}(0),b^H_{n,\tau}(0)\}^{\mathrm{T}}=\{0,0\}^{\mathrm{T}}, \tag{51}$$

where

$$\zeta_{1_n}=(1+(n\pi\mu)^2)(1+(n\pi\gamma_2)^2),\quad \zeta_{2_n}=-\gamma_1^2((n\pi)+\mu^2(n\pi)^3),$$

$$\zeta_{3_n}=-\gamma_6^2((n\pi)+\mu^2(n\pi)^3),\quad \zeta_{4_n}=1+(n\pi\mu)^2,$$

$$\eta_{1_n}=(n\pi)^2\gamma_3^2+(n\pi)^4,\quad \eta_{2_n}=(n\pi)\gamma_3^2-(n\pi)^3\gamma_4^2,$$

$$\eta_{3_n}=(n\pi)\gamma_7^2-(n\pi)^3\gamma_9^2,\quad \eta_{4_n}=\gamma_7^2+(n\pi)^2\gamma_8^2,$$

$$\beta_n^H=2\bar{f}^H(1+(n\pi\mu)^2),\quad g_n^H=\frac{n\pi v l_b}{\alpha}\sqrt{\frac{I_0}{J_6}}. \tag{52}$$

The Laplace transform is employed for solving Eq. (50) in the time domain. Hence,

$$\mathcal{L}(a_n^H)=\frac{1}{\Delta_n^H(s)}\frac{\beta_n^H g_n^H(\zeta_{4_n}s^2+\eta_{4_n})}{(s^2+(g_n^H)^2)},$$

$$\mathcal{L}(b_n^H)=-\frac{1}{\Delta_n^H(s)}\frac{\beta_n^H g_n^H(\zeta_{3_n}s^2+\eta_{3_n})}{(s^2+(g_n^H)^2)}, \tag{53}$$

where

$$\Delta_n^H(s)=(\zeta_{1_n}\zeta_{4_n}-\zeta_{2_n}\zeta_{3_n})s^4+(\zeta_{1_n}\eta_{4_n}+\eta_{1_n}\zeta_{4_n}-\zeta_{2_n}\eta_{3_n}-\eta_{2_n}\zeta_{3_n})s^2+\eta_{1_n}\eta_{4_n}-\eta_{2_n}\eta_{3_n}, \tag{54}$$

it can readily be shown that $\Delta_n^H(s)$ could be expressed as $(\zeta_{1_n}\zeta_{4_n}-\zeta_{2_n}\zeta_{3_n})(s^2+(r_{1_n}^H)^2)(s^2+(r_{2_n}^H)^2)$ where

$$r_{1_n}^H=\sqrt{\frac{(\zeta_{1_n}\eta_{4_n}+\zeta_{4_n}\eta_{1_n}-\zeta_{2_n}\eta_{3_n}-\zeta_{3_n}\eta_{2_n})-\sqrt{\chi_n}}{2(\zeta_{1_n}\zeta_{4_n}-\zeta_{2_n}\zeta_{3_n})}},$$

$$r_{2_n}^H=\sqrt{\frac{(\zeta_{1_n}\eta_{4_n}+\zeta_{4_n}\eta_{1_n}-\zeta_{2_n}\eta_{3_n}-\zeta_{3_n}\eta_{2_n})+\sqrt{\chi_n}}{2(\zeta_{1_n}\zeta_{4_n}-\zeta_{2_n}\zeta_{3_n})}}, \tag{55}$$

in which

$$\chi_n=(\zeta_{1_n}\eta_{4_n}+\eta_{1_n}\zeta_{4_n}-\zeta_{2_n}\eta_{3_n}-\eta_{2_n}\zeta_{3_n})^2-4(\eta_{1_n}\eta_{4_n}-\eta_{2_n}\eta_{3_n})(\zeta_{1_n}\zeta_{4_n}-\zeta_{2_n}\zeta_{3_n}). \tag{56}$$

Subsequently, the dynamic deflection and rotation fields of the nanotube structure modeled based on the NHOBT are derived during the course of excitation as follows:

$$\overline{w}^H(\xi,\tau)=\sum_{n=1}^{\infty}\left[\frac{A^H_{1_n}}{r^H_{1_n}}\sin(r^H_{1_n}\tau)+\frac{A^H_{2_n}}{r^H_{2_n}}\sin(r^H_{2_n}\tau)+\frac{A^H_{3_n}}{g^H_n}\sin(g^H_n\tau)\right]\sin(n\pi\xi),$$

$$\overline{\psi}^H(\xi,\tau)=\sum_{n=1}^{\infty}\left[\frac{B^H_{1_n}}{r^H_{1_n}}\sin(r^H_{1_n}\tau)+\frac{B^H_{2_n}}{r^H_{2_n}}\sin(r^H_{2_n}\tau)+\frac{B^H_{3_n}}{g^H_n}\sin(g^H_n\tau)\right]\cos(n\pi\xi), \tag{57}$$

where

$$A^H_{1_n}=\frac{\beta^H_n g^H_n(\zeta_{3_n}(r^H_{1_n})^2-\eta_{3_n})}{((r^H_{1_n})^2-(r^H_{2_n})^2)((g^H_n)^2-(r^H_{1_n})^2)(\zeta_{1_n}\zeta_{3_n}-\zeta^2_{2_n})},$$

$$A^H_{2_n}=-\frac{\beta^H_n g^H_n(\zeta_{3_n}(r^H_{2_n})^2-\eta_{3_n})}{((r^H_{1_n})^2-(r^H_{2_n})^2)((g^H_n)^2-(r^H_{2_n})^2)(\zeta_{1_n}\zeta_{3_n}-\zeta^2_{2_n})},$$

$$A^H_{3_n}=-\frac{\beta^H_n g^H_n(\zeta_{3_n}(g^H_n)^2-\eta_{3_n})}{((g^H_n)^2-(r^H_{1_n})^2)(g^2_H-(r^H_{2_n})^2)(\zeta_{1_n}\zeta_{3_n}-\zeta^2_{2_n})},$$

$$B^H_{1_n}=-\frac{\beta^H_n g^H_n(\zeta_{2_n}(r^H_{1_n})^2-\eta_{2_n})}{((r^H_{1_n})^2-(r^H_{2_n})^2)((g^H_n)^2-(r^H_{2_n})^2)(\zeta_{1_n}\zeta_{3_n}-\zeta^2_{2_n})},$$

$$B^H_{2_n}=\frac{\beta^H_n g^H_n(\zeta_{2_n}(r^H_{2_n})^2-\eta_{2_n})}{((r^H_{1_n})^2-(r^H_{2_n})^2)((g^H_n)^2-(r^H_{2_n})^2)(\zeta_{1_n}\zeta_{3_n}-\zeta^2_{2_n})},$$

$$B^H_{3_n}=\frac{\beta^H_n g^H_n(\zeta_{2_n}(g^H_n)^2-\eta_{2_n})}{((g^H_n)^2-(r^H_{1_n})^2)((g^H_n)^2-(r^H_{2_n})^2)(\zeta_{1_n}\zeta_{3_n}-\zeta^2_{2_n})}. \tag{58}$$

The equations of motion of the problem during the course of free vibration are obtained from Eq. (50) by setting $\beta^H_n=0$

$$\begin{bmatrix}\zeta_{1_n} & \zeta_{2_n}\\ \zeta_{3_n} & \zeta_{4_n}\end{bmatrix}\begin{Bmatrix}a^H_{n,\tau\tau}\\ b^H_{n,\tau\tau}\end{Bmatrix}+\begin{bmatrix}\eta_{1_n} & \eta_{2_n}\\ \eta_{3_n} & \eta_{4_n}\end{bmatrix}\begin{Bmatrix}a^H_n\\ b^H_n\end{Bmatrix}=\begin{Bmatrix}0\\ 0\end{Bmatrix},\quad \tau>\tau^H_f \tag{59}$$

with the initial conditions

$$a^H_n(\tau^H_f)=W^H_n=\frac{A^H_{1_n}}{r^H_{1_n}}\sin(r^H_{1_n}\tau^H_f)+\frac{A^H_{2_n}}{r^H_{2_n}}\sin(r^H_{2_n}\tau^H_f)+\frac{A^H_{3_n}}{g^H_n}\sin(g^H_n\tau^H_f),$$

$$b^H_n(\tau^H_f)=\Psi^H_n=\frac{B^H_{1_n}}{r^H_{1_n}}\sin(r^H_{1_n}\tau^H_f)+\frac{B^H_{2_n}}{r^H_{2_n}}\sin(r^H_{2_n}\tau^H_f)+\frac{B^H_{3_n}}{g^H_n}\sin(g^H_n\tau^H_f), \tag{60}$$

and

$$a^H_{n,\tau}(\tau^H_f)=\dot{W}^H_n=A^H_{1_n}\cos(r^H_{1_n}\tau^H_f)+A^H_{2_n}\cos(r^H_{2_n}\tau^H_f)+A^H_{3_n}\cos(g^H_n\tau^H_f),$$

$$b^H_{n,\tau}(\tau^H_f)=\dot{\Psi}^H_n=B^H_{1_n}\cos(r^H_{1_n}\tau^H_f)+B^H_{2_n}\cos(r^H_{2_n}\tau^H_f)+B^H_{3_n}\cos(g^H_n\tau^H_f), \tag{61}$$

in which $\tau^H_f=(\alpha/\nu l_b)\sqrt{J_6/I_0}$. The Laplace transform is adopted for solving the set of ODEs in Eq. (59)

$$\mathcal{L}(a^H_n)=\frac{1}{\Delta^H_n(s)}\{[(sW^H_n+\dot{W}^H_n)\zeta_{1_n}+(s\Psi^H_n+\dot{\Psi}_n)\zeta_{2_n}](\zeta_{4_n}s^2+\eta_{4_n})-[(sW_n+\dot{W}_n)\zeta_{3_n}+(s\Psi^H_n+\dot{\Psi}^H_n)\zeta_{4_n}](\zeta_{2_n}s^2+\eta_{2_n})\},$$

$$\mathcal{L}(b^H_n)=\frac{1}{\Delta^H_n(s)}\{[(sW^H_n+\dot{W}^H_n)\zeta_{3_n}+(s\Psi^H_n+\dot{\Psi}_n)\zeta_{4_n}](\zeta_{1_n}s^2+\eta_{1_n})-[(sW_n+\dot{W}_n)\zeta_{1_n}+(s\Psi^H_n+\dot{\Psi}^H_n)\zeta_{2_n}](\zeta_{3_n}s^2+\eta_{3_n})\}. \tag{62}$$

The polynomials in the denominators of $\mathcal{L}(a^H_n)$ and $\mathcal{L}(b^H_n)$ are one order higher than those in their numerators; hence, the expressions in Eq. (62) could be rewritten in the more common forms which makes taking the inverse Laplace transform more easier

$$\mathcal{L}(a^H_n)=\frac{A'^H_{1_n}}{s^2+(r^H_{1_n})^2}+\frac{A'^H_{2_n}}{s^2+(r^H_{2_n})^2}+\frac{A'^H_{3_n}s}{s^2+(r^H_{1_n})^2}+\frac{A'^H_{4_n}s}{s^2+(r^H_{2_n})^2},$$

$$\mathcal{L}(b_n^H)=\frac{B_{1_n}^{'H}}{s^2+(r_{1_n}^H)^2}+\frac{B_{2_n}^{'H}}{s^2+(r_{2_n}^H)^2}+\frac{B_{3_n}^{'H}s}{s^2+(r_{1_n}^H)^2}+\frac{B_{4_n}^{'H}s}{s^2+(r_{2_n}^H)^2}, \tag{63}$$

where

$$A_{1_n}^{'H}=\frac{1}{U}(\mathcal{A}_{4_n}-\mathcal{A}_{2_n}(r_{1_n}^H)^2),\quad B_{1_n}^{'H}=\frac{1}{U}(\mathcal{B}_{4_n}-\mathcal{B}_{2n}(r_{1_n}^H)^2),$$

$$A_{2_n}^{'H}=-\frac{1}{U}(\mathcal{A}_{4_n}-\mathcal{A}_{2_n}(r_{2_n}^H)^2),\quad B_{2_n}^{'H}=-\frac{1}{U}(\mathcal{B}_{4_n}-\mathcal{B}_{2n}(r_{2_n}^H)^2),$$

$$A_{3_n}^{'H}=\frac{1}{U}(\mathcal{A}_{3_n}-\mathcal{A}_{1_n}(r_{1_n}^H)^2),\quad B_{3_n}^{'H}=\frac{1}{U}(\mathcal{B}_{3_n}-\mathcal{B}_{1n}(r_{1_n}^H)^2),$$

$$A_{4_n}^{'H}=-\frac{1}{U}(\mathcal{A}_{3_n}-\mathcal{A}_{1_n}(r_{2_n}^H)^2),\quad B_{4_n}^{'H}=-\frac{1}{U}(\mathcal{B}_{3_n}-\mathcal{B}_{1n}(r_{2_n}^H)^2), \tag{64}$$

in which

$$U=((r_{2_n}^H)^2-(r_{1_n}^H)^2)(\zeta_{1_n}\zeta_{4_n}-\zeta_{2_n}\zeta_{3_n}),$$

$$\mathcal{A}_{1_n}=\zeta_{4_n}(\zeta_{1_n}W_n^H+\zeta_{2_n}\Psi_n^H)-\zeta_{2_n}(\zeta_{3_n}W_n^H+\zeta_{4_n}\Psi_n^H),$$

$$\mathcal{A}_{2_n}=\zeta_{4_n}(\zeta_{1_n}\dot{W}_n^H+\zeta_{2_n}\dot{\Psi}_n^H)-\zeta_{2_n}(\zeta_{3_n}\dot{W}_n^H+\zeta_{4_n}\dot{\Psi}_n^H),$$

$$\mathcal{A}_{3_n}=\eta_{4_n}(\zeta_{1_n}W_n^H+\zeta_{2_n}\Psi_n^H)-\eta_{2_n}(\zeta_{3_n}W_n^H+\zeta_{4_n}\Psi_n^H),$$

$$\mathcal{A}_{4_n}=\eta_{4_n}(\zeta_{1_n}\dot{W}_n^H+\zeta_{2_n}\dot{\Psi}_n^H)-\eta_{2_n}(\zeta_{3_n}\dot{W}_n^H+\zeta_{4_n}\dot{\Psi}_n^H),$$

$$\mathcal{B}_{1_n}=\zeta_{1_n}(\zeta_{3_n}W_n^H+\zeta_{4_n}\Psi_n^H)-\zeta_{3_n}(\zeta_{1_n}W_n^H+\zeta_{2_n}\Psi_n^H),$$

$$\mathcal{B}_{2_n}=\zeta_{1_n}(\zeta_{3_n}\dot{W}_n^H+\zeta_{4_n}\dot{\Psi}_n^H)-\zeta_{3_n}(\zeta_{1_n}\dot{W}_n^H+\zeta_{2_n}\dot{\Psi}_n^H),$$

$$\mathcal{B}_{3_n}=\eta_{1_n}(\zeta_{3_n}W_n^H+\zeta_{4_n}\Psi_n^H)-\eta_{3_n}(\zeta_{1_n}W_n^H+\zeta_{2_n}\Psi_n^H),$$

$$\mathcal{B}_{4_n}=\eta_{1_n}(\zeta_{3_n}\dot{W}_n^H+\zeta_{4_n}\dot{\Psi}_n^H)-\eta_{3_n}(\zeta_{1_n}\dot{W}_n^H+\zeta_{2_n}\dot{\Psi}_n^H). \tag{65}$$

The dynamic response of the NHOB could be readily obtained during the course of free vibration by applying inverse Laplace transform to Eq. (63):

$$\overline{w}^H(\xi,\tau)=\sum_{n=1}^{\infty}\left[\frac{A_{1_n}^{'H}}{r_{1_n}^H}\sin(r_{1_n}^H\tau')+\frac{A_{2_n}^{'H}}{r_{2_n}^H}\sin(r_{2_n}^H\tau')+A_{3_n}^{'H}\cos(r_{1_n}^H\tau')+A_{4_n}^{'H}\cos(r_{2_n}^H\tau')\right]\sin(n\pi\xi),$$

$$\overline{\psi}^H(\xi,\tau)=\sum_{n=1}^{\infty}\left[\frac{B_{1_n}^{'H}}{r_{1_n}^H}\sin(r_{1_n}^H\tau')+\frac{B_{2_n}^{'H}}{r_{2_n}^H}\sin(r_{2_n}^H\tau')+B_{3_n}^{'H}\cos(r_{1_n}^H\tau')+B_{4_n}^{'H}\cos(r_{2_n}^H\tau')\right]\cos(n\pi\xi), \tag{66}$$

in which $\tau'=\tau-\tau_f^H$.

4.4. Special cases

In this part, Eqs. (12), (27) and (50) are studied for some special cases of vibration of the nanotube structure acted upon by a moving nanoparticle.

4.4.1. $v=0$ *(The static analysis)*

If we set $g_n^E\tau=g_n^T\tau=g_n^H\tau=\xi_m$ and $g_n^E=g_n^T=g_n^H=0$ in Eqs. (12), (27) and (50), then the dimensionless static deflection and rotation fields of various nonlocal beam theories due to the point loading of the nanoparticle weight at the point ξ_m are obtained as

$$\overline{w}^E(\xi,\tau)=\sum_{n=1}^{\infty}\frac{\beta_n^E}{(r_n^E)^2}\sin(n\pi\xi_m)\sin(n\pi\xi),$$

$$\overline{w}_{,\xi}^E(\xi,\tau)=\sum_{n=1}^{\infty}\frac{n\pi\beta_n^E}{(r_n^E)^2}\sin(n\pi\xi_m)\cos(n\pi\xi), \tag{67}$$

$$\overline{w}^{\mathrm{T}}(\xi,\tau)=\sum_{n=1}^{\infty}\frac{\beta_n^{\mathrm{T}}\varsigma_{4_n}}{(r_{1_n}^{\mathrm{T}}r_{2_n}^{\mathrm{T}})^2}\sin(n\pi\xi_m)\sin(n\pi\xi),$$

$$\overline{\theta}^{\mathrm{T}}(\xi,\tau)=\sum_{n=1}^{\infty}\frac{\beta_n^{\mathrm{T}}\varsigma_{3_n}}{(r_{1_n}^{\mathrm{T}}r_{2_n}^{\mathrm{T}})^2}\sin(n\pi\xi_m)\cos(n\pi\xi),\tag{68}$$

$$\overline{w}^{H}(\xi,\tau)=\sum_{n=1}^{\infty}\frac{\beta_n^{H}\eta_{3_n}}{(\zeta_{2_n}^2-\zeta_{1_n}\zeta_{3_n})(r_{1_n}^{H}r_{2_n}^{H})^2}\sin(n\pi\xi_m)\sin(n\pi\xi),$$

$$\overline{\psi}^{H}(\xi,\tau)=-\sum_{n=1}^{\infty}\frac{\beta_n^{H}\eta_{2_n}}{(\zeta_{2_n}^2-\zeta_{1_n}\zeta_{3_n})(r_{1_n}^{H}r_{2_n}^{H})^2}\sin(n\pi\xi_m)\cos(n\pi\xi).\tag{69}$$

Moreover, the static bending moment of various beams could easily be obtained by substituting Eqs. (67)–(69) into Eqs. (11), (26) and (49).

4.4.2. $g_m^{[\,]}=r_{i_m}^{[\,]}([\,]=E$ or T or $H, i=1$ or $2, m\geq 1)$ *(The critical velocities)*

In this case, Eqs. (15), (30) and (53) could not be utilized directly for capturing the dynamic response of the nanotube structure because the denominators of these equations take zero values; therefore, these equations should be reconstructed from the original expressions before applying the Laplace transform. In the case of $g_m^{[\,]}=r_{i_m}^{[\,]}$, the expressions of Eqs. (15), (30) and (53) are rewritten as

$$\mathcal{L}(a_m^E)=\frac{\beta_m^E g_m^E}{(s^2+(g_m^E)^2)^2},\tag{70}$$

$$\mathcal{L}(a_m^{\mathrm{T}})=\frac{\beta_m^{\mathrm{T}} g_m^{\mathrm{T}}(s^2+\varsigma_{4_m})}{(s^2+(r_{2_m}^{\mathrm{T}})^2)(s^2+(r_{1_m}^{\mathrm{T}})^2)^2},$$

$$\mathcal{L}(b_m^{\mathrm{T}})=-\frac{\beta_m^{\mathrm{T}} g_m^{\mathrm{T}}(s^2+\varsigma_{3_m})}{(s^2+(r_{2_m}^{\mathrm{T}})^2)(s^2+(r_{1_m}^{\mathrm{T}})^2)^2},\tag{71}$$

$$\mathcal{L}(a_m^H)=\frac{\beta_m^H g_m^H(\zeta_{4_m}s^2+\eta_{4_m})}{(\zeta_{1_n}\zeta_{4_m}-\zeta_{2_m}\zeta_{3_m})(s^2+(r_{2_m}^H)^2)(s^2+(r_{1_m}^H)^2)^2},$$

$$\mathcal{L}(b_m^H)=-\frac{\beta_m^H g_m^H(\zeta_{3_m}s^2+\eta_{3_m})}{(\zeta_{1_n}\zeta_{4_m}-\zeta_{2_m}\zeta_{3_m})(s^2+(r_{2_m}^H)^2)(s^2+(r_{1_m}^H)^2)^2}.\tag{72}$$

Using the Laplace transform, the nonlocal deflection fields are obtained as the following during the course of excitation:

$$\overline{w}^{E}(\xi,\tau)=\frac{\beta_m^E g_m^E}{2(r_m^E)^2}[\sin(r_m^E\tau)-r_m^E\tau\cos(r_m^E\tau)]\sin(m\pi\xi)+\sum_{n=1,n\neq m}^{\infty}\frac{\beta_n^E}{r_n^E((g_n^E)^2-(r_n^E)^2)}[g_n^E\sin(r_n^E\tau)-r_n^E\sin(g_n^E\tau)]\sin(n\pi\xi),$$

$$\overline{w}_{,\xi}^{E}(\xi,\tau)=\frac{m\pi\beta_m^E g_m^E}{2(r_m^E)^2}[\sin(r_m^E\tau)-r_m^E\tau\cos(r_m^E\tau)]\cos(m\pi\xi)+\sum_{n=1,n\neq m}^{\infty}\frac{n\pi\beta_n^E}{r_n^E((g_n^E)^2-(r_n^E)^2)}[g_n^E\sin(r_n^E\tau)-r_n^E\sin(g_n^E\tau)]\cos(n\pi\xi),\tag{73}$$

$$\overline{w}^{\mathrm{T}}(\xi,\tau)=\beta_m^{\mathrm{T}}g_m^{\mathrm{T}}\left[\frac{((r_{1_m}^{\mathrm{T}})^4+(r_{1_m}^{\mathrm{T}})^2(r_{2_m}^{\mathrm{T}})^2-3(r_{1_m}^{\mathrm{T}})^2\varsigma_{4_m}+(r_{2_m}^{\mathrm{T}})^2\varsigma_{4_m})}{2(r_{1_m}^{\mathrm{T}})^3((r_{1_m}^{\mathrm{T}})^2-(r_{2_m}^{\mathrm{T}})^2)^2}\sin(r_{1_m}^{\mathrm{T}}\tau)-\frac{\tau}{2(r_{1_m}^{\mathrm{T}})^2(r_{1_m}^{\mathrm{T}}2-r_{2_m}^{\mathrm{T}}2)}\cos(r_{1_m}^{\mathrm{T}}\tau)\right.$$
$$\left.+\frac{(r_{2_m}^{\mathrm{T}})^2-\varsigma_{4_m}}{r_{2_m}^{\mathrm{T}}((r_{1_m}^{\mathrm{T}})^2-(r_{2_m}^{\mathrm{T}})^2)^2}\sin(r_{2_m}^{\mathrm{T}}\tau)\right]\sin(m\pi\xi)+\sum_{n=1,n\neq m}^{\infty}\left[\frac{A_{1_n}^{\mathrm{T}}}{r_{1_n}^{\mathrm{T}}}\sin(r_{1_n}^{\mathrm{T}}\tau)+\frac{A_{2_n}^{\mathrm{T}}}{r_{2_n}^{\mathrm{T}}}\sin(r_{2_n}^{\mathrm{T}}\tau)+\frac{A_{3_n}^{\mathrm{T}}}{g_n^{\mathrm{T}}}\sin(g_n^{\mathrm{T}}\tau)\right]\sin(n\pi\xi),$$

$$\overline{\theta}^{\mathrm{T}}(\xi,\tau)=\beta_m^{\mathrm{T}}g_m^{\mathrm{T}}\varsigma_{3_m}\left[\frac{3(r_{1_m}^{\mathrm{T}})^2-(r_{2_m}^{\mathrm{T}})^2}{2(r_{1_m}^{\mathrm{T}})^3((r_{1_m}^{\mathrm{T}})^2-(r_{2_m}^{\mathrm{T}})^2)^2}\sin(r_{1_m}^{\mathrm{T}}\tau)-\frac{\tau}{2(r_{1_m}^{\mathrm{T}})^2((r_{1_m}^{\mathrm{T}})^2-(r_{2_m}^{\mathrm{T}})^2)}\cos(r_{1_m}^{\mathrm{T}}\tau)-\frac{1}{r_{1_m}^{\mathrm{T}}((r_{1_m}^{\mathrm{T}})^2-(r_{2_m}^{\mathrm{T}})^2)^2}\sin(r_{2_m}^{\mathrm{T}}\tau)\right]\cos(m\pi\xi)$$
$$+\sum_{n=1,n\neq m}^{\infty}\left[\frac{B_{1_n}^{\mathrm{T}}}{r_{1_n}^{\mathrm{T}}}\sin(r_{1_n}^{\mathrm{T}}\tau)+\frac{B_{2_n}^{\mathrm{T}}}{r_{2_n}^{\mathrm{T}}}\sin(r_{2_n}^{\mathrm{T}}\tau)+\frac{B_{3_n}^{\mathrm{T}}}{g_n^{\mathrm{T}}}\sin(g_n^{\mathrm{T}}\tau)\right]\cos(n\pi\xi),\tag{74}$$

$$\overline{w}^{H}(\xi,\tau)=\frac{\beta_m^H g_m^H}{\zeta_{1_m}\zeta_{4_m}-\zeta_{2_m}\zeta_{3_m}}\left[\frac{((r_{1_m}^H)^4\zeta_{4_m}+(r_{1_m}^H)^2(r_{2_m}^H)^2\zeta_{4_m}-3(r_{1_m}^H)^2\eta_{4_m}+(r_{2_m}^H)^2\eta_{4_m})}{2(r_{1_m}^H)^3((r_{1_m}^H)^2-(r_{2_m}^H)^2)^2}\sin(r_{1_m}^H\tau)\right.$$

$$+\frac{\eta_{4_m}-\zeta_{4_m}(r_{1_m}^H)^2}{2(r_{1_m}^H)^2((r_{1_m}^H)^2-(r_{2_m}^H)^2)}\tau\cos(r_{1_m}^H\tau)+\frac{(r_{2_m}^H)^2\zeta_{4_m}-\eta_{4_m}}{r_{2_m}^H((r_{1_m}^H)^2-(r_{2_m}^H)^2)^2}\sin(r_{2_m}^H\tau)\Bigg]\sin(m\pi\xi)$$
$$+\sum_{n=1,n\neq m}^{\infty}\left[\frac{A_{1_n}^H}{r_{1_n}^H}\sin(r_{1_n}^H\tau)+\frac{A_{2_n}^H}{r_{2_n}^H}\sin(r_{2_n}^H\tau)+\frac{A_{3_n}^H}{g_n^H}\sin(g_n^H\tau)\right]\sin(n\pi\xi),$$

$$\overline{\psi}^H(\xi,\tau)=-\frac{\beta_m^H g_m^H}{\zeta_{1_m}\zeta_{4_m}-\zeta_{2_m}\zeta_{3_m}}\Bigg[\frac{((r_{1_m}^H)^4\zeta_{3_m}+(r_{1_m}^H)^2(r_{2_m}^H)^2\zeta_{3_m}-3(r_{1_m}^H)^2\eta_{3_m}+(r_{2_m}^H)^2\eta_{3_m})}{2(r_{1_m}^H)^3((r_{1_m}^H)^2-(r_{2_m}^H)^2)^2}\sin(r_{1_m}^H\tau)$$
$$+\frac{\eta_{3_m}-\zeta_{3_m}(r_{1_m}^H)^2}{2(r_{1_m}^H)^2((r_{1_m}^H)^2-(r_{2_m}^H)^2)}\tau\cos(r_{1_m}^H\tau)+\frac{(r_{2_m}^H)^2\zeta_{3_m}-\eta_{3_m}}{r_{2_m}^H((r_{1_m}^H)^2-(r_{2_m}^H)^2)^2}\sin(r_{2_m}^H\tau)\Bigg]\cos(m\pi\xi)$$
$$+\sum_{n=1,n\neq m}^{\infty}\left[\frac{B_{1_n}^H}{r_{1_n}^H}\sin(r_{1_n}^H\tau)+\frac{B_{2_n}^H}{r_{2_n}^H}\sin(r_{2_n}^H\tau)+\frac{B_{3_n}^H}{g_n^H}\sin(g_n^H\tau)\right]\cos(n\pi\xi). \tag{75}$$

To obtain the dynamic response of the nanobeams during the course of free vibration, the initial conditions of the free vibration are calculated from Eqs. (73)–(75) at the dimensionless time τ_f associated with each beam theory. Additionally, the bending moment within various beam models could be readily derived by substituting Eqs. (73), (74) and (75) into Eqs. (11), (26) and (49), correspondingly.

As it is clear from Eqs. (73) to (75), the deflections and rotations of all points of the nanobeams increase with time during the course of excitation. Moreover, the terms of deflections and rotations associated with the first mode of vibration are the dominant ones over all other terms. The velocity obtained from $g_1^{[\,]}=\min(r_{1_1}^{[\,]},r_{2_1}^{[\,]})$ is defined as the critical velocity of the nanoparticle associated with the nonlocal [ ] beam. Therefore, the critical velocity for various nonlocal beam models could be calculated from

$$v_{cr}^E=\frac{v'^E}{\sqrt{(1+(\pi\mu)^2)(1+(\pi/\lambda)^2)}},$$

$$v_{cr}^{\mathrm{T}}=\frac{v'^{\mathrm{T}}}{\pi^2\sqrt{2(1+(\pi\mu)^2)}}\sqrt{\lambda^2+\pi^2+\eta\pi^2\lambda^2-\sqrt{(\lambda^2+\eta\pi^2\lambda^2-\pi^2)^2+4\pi^2\lambda^2}},$$

$$v_{cr}^H=\frac{v'^H}{\pi^2\sqrt{2(1+(\pi\mu)^2)}}\sqrt{\Sigma-\sqrt{\Sigma^2-\Upsilon}}; \tag{76}$$

where $v'^E=(\pi/l_b)\sqrt{E_bI_b/\rho_bA_b}$ [42], $v'^{\mathrm{T}}=\pi\sqrt{k_sG_b/\rho_b}$, $v'^H=(\pi\alpha/l_b)\sqrt{J_6/I_0}$ and

$$\Sigma=\gamma_7^2+\pi^2(\gamma_3^2+\gamma_8^2+\gamma_1^2\gamma_7^2+\gamma_3^2\gamma_6^2)+\pi^4(1-\gamma_1^2\gamma_9^2-\gamma_4^2\gamma_6^2),$$

$$\Upsilon=4\pi^4[1+\pi^2(\gamma_2^2-\gamma_1^2\gamma_6^2)][\gamma_7^2+\gamma_3^2\gamma_8^2+\gamma_3^2\gamma_9^2+\gamma_4^2\gamma_7^2+\pi^2(\gamma_8^2-\gamma_4^2\gamma_9^2)]. \tag{77}$$

Eq. (76) states that the critical velocity is somehow inversely proportional to the normalized scale effect parameter; nevertheless, the critical velocity magnifies with the slenderness ratio of the ECS.

4.4.3. $\bar{f}^{[\,]}=0$ (The natural frequencies)

In this case, the set of equations of motion associated with the nonlocal [ ] beam theory could be expressed as

$$\mathbf{M}^{[\,]}\mathbf{x}_{,\tau\tau}^{[\,]}+\mathbf{K}^{[\,]}\mathbf{x}^{[\,]}=\mathbf{0}. \tag{78}$$

It is presumed that $\mathbf{x}^{[\,]}(\tau)=\tilde{\mathbf{x}}_0^{[\,]}e^{i\varpi^{[\,]}\tau}$ where $\varpi^{[\,]}$ is the nondimensional frequency corresponding to the natural frequency of the nonlocal [ ] beam theory, $\omega^{[\,]}$. By substituting the equivalent expression of $\mathbf{x}^{[\,]}(\tau)$ into Eq. (78)

$$\left[-(\varpi^{[\,]})^2\mathbf{M}^{[\,]}+\mathbf{K}^{[\,]}\right]\tilde{\mathbf{x}}_0^{[\,]}=\mathbf{0}, \tag{79}$$

and by solving this set of eigenvalue equations, eigenvalues (natural frequencies) and eigenvectors (modes of free vibration) of the nanobeams are obtained. For the sake of more comparability of the obtained results with each other, a dimensionless frequency associated with the n th mode of vibration of nonlocal [ ] beam theory is defined as $\Omega_n^{[\,]}=((\rho_bA_b/E_bI_b)\varpi_n^{[\,]2})^{1/4}$ in which $\varpi_n^{[\,]}=\min(r_{1_n}^{[\,]},r_{2_n}^{[\,]})$; therefore,

$$\Omega_n^E=\sqrt{\varpi_n^E},$$

$$\Omega_n^{\mathrm{T}}=\eta^{-1/4}\sqrt{\varpi_n^{\mathrm{T}}},$$

Table 1
Study of the first five dimensionless frequencies of the NEB, NTB and NHOB for different values of slenderness ratio and scale effect parameter of the ECS.

λ	$\mu=0.0$			$\mu=0.1$			$\mu=0.2$			$\mu=0.3$		
(l_b/D_o)[a]	NEBT	NTBT	NHOBT	NEBT	NTBT	NHOBT	NEBT	NTBT	NHOBT	NEBT	NTBT	NHOBT
10	3.0685	2.8289	2.9083	2.9972	2.7631	2.8407	2.8236	2.6031	2.6762	2.6177	2.4132	2.4810
(3.35)	5.7817	4.7900	5.0856	5.3202	4.4077	4.6796	4.5623	3.7798	4.0130	3.9580	3.2792	3.4815
	8.0400	6.2211	6.7448	6.8587	5.3070	5.7538	5.5040	4.2588	4.6174	4.6426	3.5923	3.8947
	9.9161	7.3692	8.1049	7.8248	5.8150	6.3956	6.0293	4.4807	4.9280	5.0210	3.7314	4.1039
	11.5112	8.3479	9.2818	8.4356	6.1175	6.8019	6.3397	4.5975	5.1118	5.2446	3.8034	4.2289
30	3.1330	3.0957	3.1093	3.0602	3.0237	3.0370	2.8830	2.8486	2.8611	2.6727	2.6408	2.6524
(10.05)	6.2161	5.9572	6.0475	5.7199	5.4817	5.5648	4.9051	4.7009	4.7721	4.2554	4.0782	4.1400
	9.2056	8.4866	8.7250	7.8530	7.2397	7.4430	6.3020	5.8098	5.9729	5.3157	4.9005	5.0381
	12.0686	10.6972	11.1318	9.5233	8.4411	8.7841	7.3381	6.5042	6.7684	6.1110	5.4165	5.6366
	14.7848	12.6407	13.2964	10.8346	9.2634	9.7439	8.1426	6.9617	7.3229	6.7361	5.7593	6.0580
50	3.1385	3.1246	3.1297	3.0655	3.0519	3.0569	2.8880	2.8752	2.8799	2.6774	2.6655	2.6699
(16.76)	6.2586	6.1535	6.1915	5.7591	5.6623	5.6973	4.9387	4.8557	4.8857	4.2845	4.2126	4.2386
	9.3429	9.0175	9.1321	7.9701	7.6925	7.7903	6.3959	6.1732	6.2516	5.3950	5.2071	5.2732
	12.3754	11.6828	11.9195	9.7654	9.2189	9.4056	7.5246	7.1035	7.2474	6.2663	5.9156	6.0354
	15.3427	14.1444	14.5416	11.2434	10.3653	10.6564	8.4498	7.7899	8.0086	6.9903	6.4444	6.6254
70	3.1400	3.1328	3.1355	3.0670	3.0600	3.0626	2.8894	2.8828	2.8852	2.6786	2.6725	2.6748
(23.46)	6.2706	6.2150	6.2353	5.7701	5.7189	5.7376	4.9481	4.9042	4.9203	4.2927	4.2546	4.2686
	9.3825	9.2035	9.2680	8.0040	7.8512	7.9062	6.4231	6.3005	6.3447	5.4179	5.3144	5.3517
	12.4671	12.0681	12.2092	9.8378	9.5229	9.6343	7.5804	7.3377	7.4235	6.3127	6.1107	6.1821
	15.5162	14.7920	15.0427	11.3706	10.8399	11.0236	8.5454	8.1465	8.2846	7.0694	6.7394	6.8537

[a] Note: The parameter D_o denotes the outer diameter of the nanotube structure.

$$\Omega_n^H=\left(\frac{\alpha^2 J_6\rho_b A_b}{I_0 E_b I_b}\right)^{1/4}\sqrt{\varpi_n^H}. \tag{80}$$

The obtained results of the first five dimensionless frequencies of various nonlocal beam models have been presented in Table 1 for different values of the slenderness ratio of the ECS and normalized scale effect parameter. The results show that an increase in the scale effect would result in the decrease of dimensionless frequencies regardless of the assumed nonlocal beam theory and slenderness ratio of the ECS. Furthermore, the difference between dimensionless frequencies of each pair of nonlocal beams increases as the slenderness ratio of the ECS decreases, particularly for high values of the scale effect parameter; however, this difference generally magnifies as the mode number becomes greater.

5. Numerical results

This section presents results of dynamic deflection of nanotube structures simulated based on the NEBT, NTBT and NHOBT under excitation of a moving nanoparticle. The analytical expressions obtained for dynamic deflection of various beam models will be plotted in terms of time to show the capability of each beam theory in predicting the dynamic response of the ECS under a moving nanoparticle. Moreover, the effects of the scale effect parameter, the slenderness ratio of the ECS and velocity of the moving nanoparticle on the time history of deflection as well as maximum dynamic deflection of various nonlocal beams are discussed in some detail. To this end, consider the ECS of a SWCNT with the following data: $r_m=3.0$, $t_b=0.34$ nm, $\rho_b=2500\,\mathrm{kg/m^3}$, $E_b=1$ TPa, $\nu_b=0.2$ [14] and the shear modulus is determined from $G_b=0.5\,E_b/(1+\nu_b)$. For the numerical calculations, the normalized dimensionless deflection $w_N=\overline{w}(x,t)/(mgl_b^2/(48E_bI_b))$ and the normalized velocity of the moving nanoparticle $V_N=v/v_{cr}^E$ are utilized. The other needed parameters are evaluated based on the geometry of the cross-section of the ECS as (see Fig. 1(b))

$$A_b=\pi(r_o^2-r_i^2),\quad I_b=\pi(r_o^4-r_i^4)/4,\quad \kappa=G_b\pi(r_o^2-r_i^2)/2,\quad \alpha=1/(3r_o^2),$$

$$I_0=\rho_b A_b,\quad I_2=\rho_b\pi(r_o^4-r_i^4)/4,\quad I_4=\rho_b\pi(r_o^6-r_i^6)/8,\quad I_6=5\rho_b\pi(r_o^8-r_i^8)/64,$$

$$J_2=E_b\pi(r_o^4-r_i^4)/4,\quad J_4=E_b\pi(r_o^6-r_i^6)/8,\quad J_6=5E_b\pi(r_o^8-r_i^8)/64. \tag{81}$$

Moreover, the shear correction factor for a tube-like Timoshenko beam is determined from the following formula [43]:

$$k_s=\frac{6(1+z^2)^2}{7+34z^2+7z^4},\quad z=\frac{r_i}{r_o}. \tag{82}$$

In Figs. 2(a–c), the time history of deflection at midspan of the ECS has been presented for various values of the slenderness ratio of the ECS and scale effect parameter based on the NEBT, NTBT and NHOBT. In all the figures, the dotted

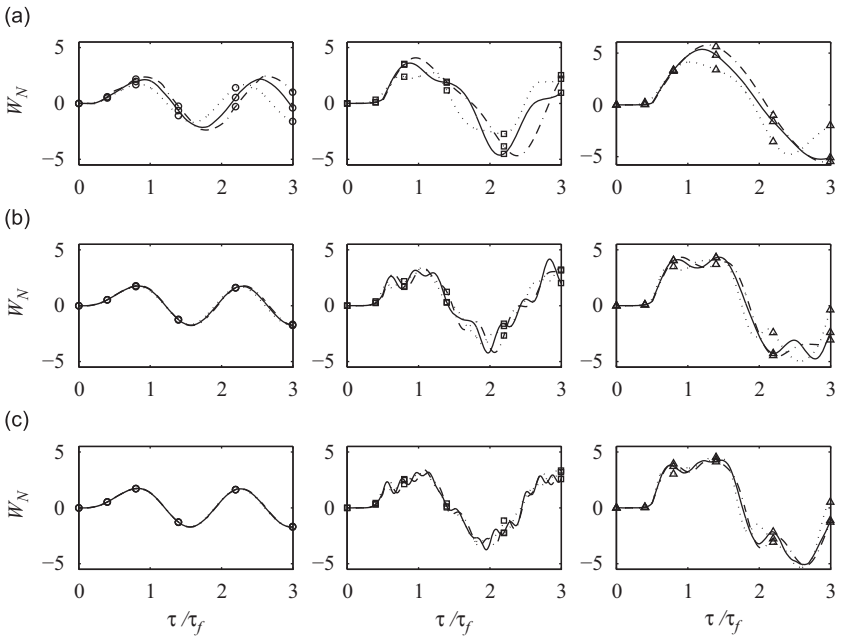

Fig. 2. Normalized dynamic deflection at midspan of the ECS for various values of slenderness ratio and scale effect parameter: (a) $\lambda = 10$, (b) $\lambda = 30$, (c) $\lambda = 50$; ((◦) $\mu = 0.0$, (□) $\mu = 0.3$, (△) $\mu = 0.5$; (...) NEBT, (−.−) NTBT, (—) NHOBT; $V_N = 0.7$).

lines, dashed lines and solid lines represent, respectively, the corresponding results of the NEB, NTB and NHOB for $V_N = 0.7$. For low values of the slenderness ratio of the ECS ($\lambda = 10$), the dynamic deflection of the NEB is obviously distinct from those of the NTB and NHOB, especially for high values of the scale effect parameter. As the slenderness ratio of the ECS increases, the difference between the results of various nonlocal beam theories becomes negligible regardless of the assumed value of the scale effect parameter. Furthermore, for a constant value of λ, an increase of the scale effect parameter would result in greater difference between the results of the NEB and those of the NTB and NHOB. Another important issue is that, the midspan deflection of the nanobeams grows substantially just after the moving nanoparticle traversed the midspan point such that the greater the scale effect parameter, the higher the maximum dynamic deflection irrespective of the presumed nonlocal beam theory. In the case of $\mu = 0.5$, the maximum dynamic deflections occur in the second phase of vibration; however, the local beam theory predicts that it would happen in the first phase of vibration.

Plots of time history of deflection at the midspan of the ECS are provided in Figs. 3(a–c) to further investigate the effect of velocity of the moving nanoparticle and scale effect on dynamic deflections of various nonlocal beam models. The results have been presented for $\lambda = 20$ and three levels of the moving nanoparticle velocity (i.e., $V_N = 0.3, 1.0, 1.5$). In the case of $\mu = 0$, except for adjacent regions of the peak points of the graphs, the results of various beam theories are close to each other such that the results of the NHOB are generally between those of the NEB and NTB for most of the time intervals. Furthermore, the midspan deflections of the NTB and the NHOB show a sharp slope just after the midpoint of the ECS is traversed by the moving nanoparticle, particularly for $V_N = 0.3$ and $\mu \geq 0.3$; nevertheless, the NEBT could never predict such a phenomenon. It means that the nonlocal shear deformable beam theories could capture some data of vibration in the nanoscale beyond the shear effect. The difference between the results of the NEB and those of the NTB and NHOB is apparent during free vibration, especially for low values of the moving nanoparticle velocity and high values of the scale effect parameter. It is clear from Figs. 3(a–c) that the occurrence of the maximum dynamic deflection moves from the first phase to the second one as the velocity of moving nanoparticle passes the critical velocity. Additionally, the maximum dynamic responses of the nanobeam models having higher scale effect parameter decrease more vigorously with velocity of the moving nanoparticle.

An important analysis is provided for the role of the moving nanoparticle velocity on the maximum dynamic deflection for different values of the slenderness ratio and scale effect parameter. For this purpose, the maximum dynamic deflection of the ECS to the maximum static deflection due to an applied point load of the magnitude mg at the midpoint of the local Euler–Bernoulli beam is defined as the dynamic amplitude factor (DAF). In Figs. 4(a–e), the DAFs of the nonlocal beams have been plotted as a function of the velocity of the moving nanoparticle for various values of λ and μ. As Fig. 4(a) shows, in the case of $\lambda = 10$, the DAFs of the NEB show remarkable difference from those of the NTB and NHOB, especially for high values of the scale effect parameter ($\mu \geq 0.3$) and low levels of moving nanoparticle velocity ($V_N < 0.4$). Moreover, the difference between the predicted DAFs by various beam models based on the local continuum theory (i.e., $\mu = 0$) becomes negligible for different values of the velocity of moving nanoparticle as the slenderness ratio increases; however, this fact is followed with a lower rate for the nonlocal beam models with higher scale effect parameter. This fact reveals that the NTBT

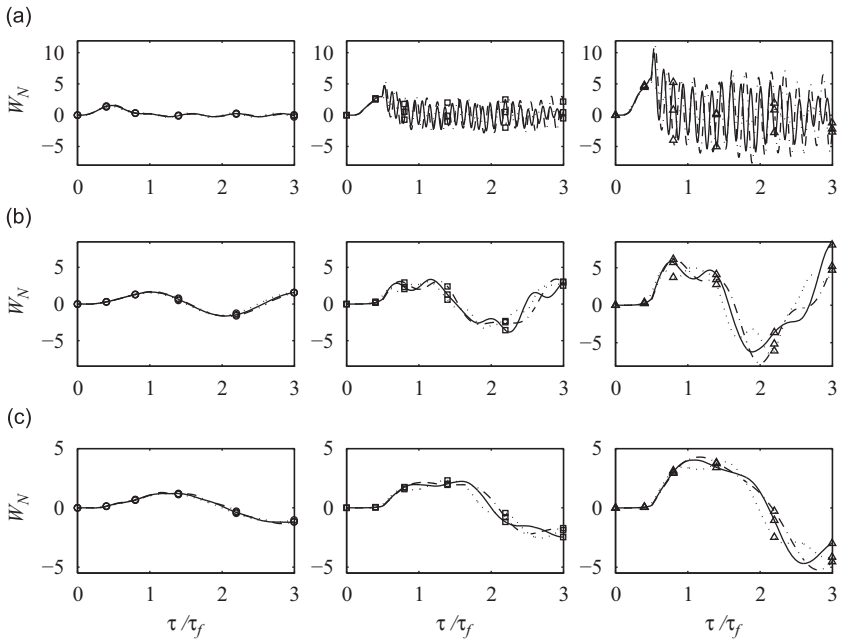

Fig. 3. Normalized dynamic deflection at midspan of the ECS for various values of moving nanoparticle velocity and scale effect parameter: (a) $V_N = 0.3$, (b) $V_N = 1.0$, (c) $V_N = 1.5$; ((◦) $\mu = 0.0$, (□) $\mu = 0.3$, (△) $\mu = 0.5$; (...) NEBT, (−.−) NTBT, (—) NHOBT; $\lambda = 20$).

and NHOBT not only introduce shear effect but also take into account additional data of the scale effect in analyzing nanotube structures under a moving nanoparticle. This result is in line with that of Wang and Liew [17] for static analysis of nanostructures under a point load as a special case of the dynamic loading (see Section 4.4.1). Equally important is that an increase of the scale effect parameter would result in a greater difference between the results of the NTB and those of the NHOB, particularly for low values of the slenderness ratio and the moving nanoparticle velocity ($\lambda \leq 30, V_N < 0.2$). In such conditions, application of the NHOBT instead of the NTBT is strictly recommended to obtain a more realistic dynamic response of the nanotube structure.

To determine the application limits of various nonlocal beams, the ranges of the normalized moving nanoparticle velocity in which the NEBT and NTBT could reproduce the DAFs of the NHOBT with the relative errors less than 5 percent and 10 percent have been summarized in Table 2. The information about this table has been provided through a close scrutiny of the demonstrated results in Figs. 4(a–e). As it is clear, for nanotube structures using local beam models with $\lambda = 10$, neither the NEBT nor the NTBT could predict the DAFs of the NHOBT with relative error less than 10 percent. However, as the effect of scale effect is highlighted, the NTBT could track the results of the NHOBT for some short ranges of V_N. In the case of local continuum beams with $\lambda \geq 30$, both the NEBT and NTBT could capture the DAFs of the NHOBT with relative error less than 5 percent for all ranges of V_N. In the case of $\mu = 0.3$, the NEBT and NTBT could not predict the results of the NHOBT with relative error lower than 5 percent for those nanotubes with $\lambda \leq 70$ and 30, respectively. For a nanotube with $\lambda = 30$ and $\mu \geq 0.3$, the NTBT could generally reproduce the DAFs of the NHOBT with relative error less than 10 percent for $V_N > 0.35$. In the cases of $\lambda = 30$ or 50 and $\mu = 0.5$, the results indicate that although the NEBT underestimates the DAFs of the NHOBT less than 10 percent just for $V_N > 0.95$, the NTBT overestimates them with similar accuracy for wide ranges of V_N. However, the NTBT is still capable of reproducing the DAFs of the NHOBT with relative error lower than 5 percent in the case of $\lambda = 30$ for some ranges of V_N. As the slenderness ratio of the nanotube structure increases, the results of the NEBT and NTBT would be close to those of the NHOBT for a wider range of V_N. For example, in the case of $\lambda = 90$ and $\mu = 0.3$, the results of the NEBT and NTBT could fairly track the DAFs of the NHOBT irrespective of V_N.

Another interesting parametric study is to investigate the effects of the scale effect parameter on the DAFs of various nonlocal beam models. In Figs. 5(a–c), the plots of the DAFs versus μ are presented for different values of the slenderness ratio as well as various levels of the velocity of the moving nanoparticle. It could be seen that an increase in the scale effect parameter would generally result in the increase of the predicted DAFs of various nonlocal beams. A brief comparison of the slope of the depicted plots in Figs. 5(a–c) reveals that the variation of the scale effect parameter for further stocky nanotube structures traversed by a moving nanoparticle with approximate velocity $0.3\, v_{cr}^{E}$ would have more effect on the variation of the predicted DAFs with respect to the other cases. Moreover, it is obvious that there is a considerable difference between the predicted DAFs by the NTBT and NHOBT with those of the NEB, particularly for very stocky nanotube structures (i.e., $\lambda = 10$). However, as the slenderness ratio of the nanotube structure increases, the differences between DAFs of all nonlocal beams as well as the predicted values of DAFs reduce regardless of the scale effect. In the case of $\lambda = 10$ (see Fig. 5(a)), neither the NTBT nor the NEBT could reproduce the DAFs of the NHOBT with relative error less than

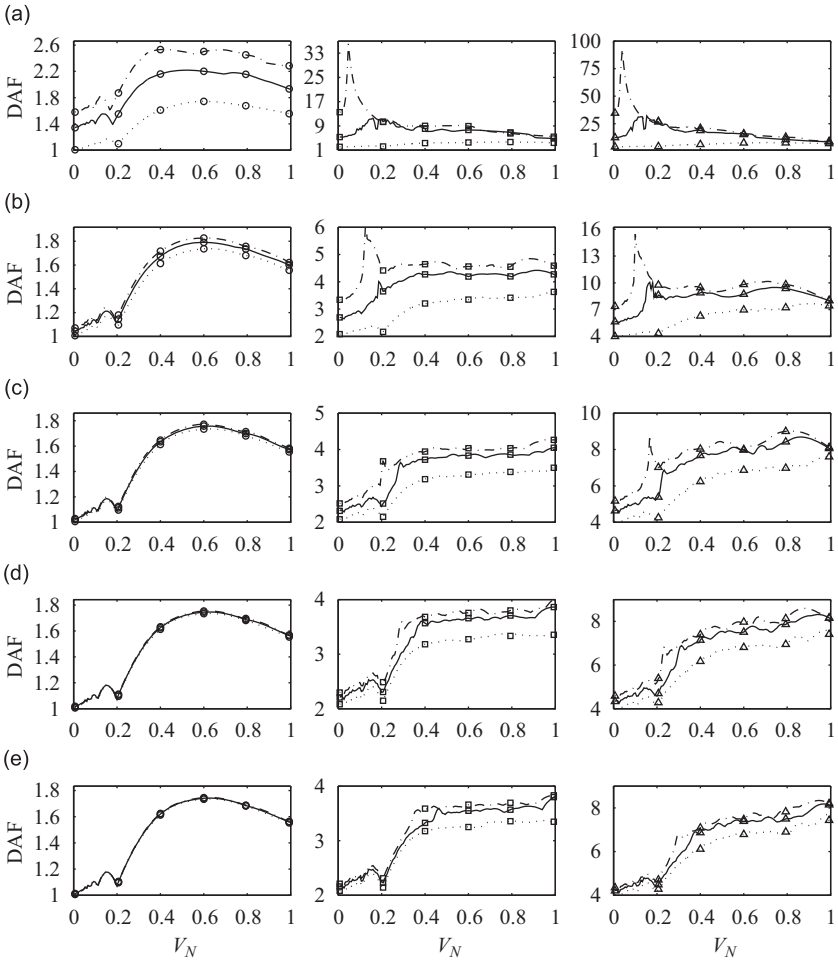

Fig. 4. Effect of the velocity of moving nanoparticle on dynamic amplitude factor of the ECS for various values of slenderness ratio and scale effect parameter: (a) $\lambda = 10$, (b) $\lambda = 30$, (c) $\lambda = 50$, (d) $\lambda = 70$, (e) $\lambda = 90$; ((◦) $\mu = 0.0$, (□) $\mu = 0.3$, (△) $\mu = 0.5$; (...) NEBT, (−.−) NTBT, (—) NHOBT).

20 percent, irrespective of the scale effect parameter. In the case of $\lambda = 30, V_N = 0.3$ (see Fig. 5(b)), the NTBT could generate the results of the NHOBT with relative error less than 15 percent for a large range of the scale effect parameter ($\mu \leq 0.08$ and $\mu \geq 0.15$), however, the NEBT could predict the results of the NHOBT with the aforementioned range of relative error just for $\mu \leq 0.15$. For $\lambda = 50, V_N = 0.3$ (see Fig. 5(c)), the NTBT could approximate the results of the NHOBT with relative error less than 10 percent for a wide range of the scale effect parameter ($\mu \leq 0.15$ and $\mu \geq 0.25$). In this case, the NEBT could predict the results of the NHOBT with the relative error less than 10 percent only for $\mu \leq 0.2$. As the velocity of the moving nanoparticle moves to a greater extent, the NEBT and NTBT could reproduce the DAFs of the NHOBT for a more extensive range of the scale effect parameter. For example, in the case of $\lambda = 50, V_N = 1$, the NTBT and NEBT could generate the DAFs of the NHOBT with relative error less than 6 percent and 10 percent, correspondingly.

For further investigation on the capabilities of the proposed nonlocal beam theories in predicting dynamic response of nanotube structures under a moving nanoparticle, the DAFs of different nonlocal beam models have been demonstrated as a function of the slenderness ratio of the EQS for various values of moving nanoparticle velocity and scale effect parameter in Figs. 6(a–d). As it is expected, for given values of V_N and μ, the DAFs of various nonlocal beam theories converge to a constant level by an increase in the slenderness ratio of the EQS. The rate of convergence would magnify with the velocity of the moving nanoparticle as the scale effect parameter would lessen. In most of the cases, the predicted DAFs by the NEBT and NTBT are, respectively, lower and higher than those obtained by the NHOBT. However, the results of the NTB and NHOB are generally in line and close to each other. In the case of $\mu = 0$, for $\lambda \leq 40$, the predicted DAFs by the NEBT in comparison to those of nonlocal shear deformable beams are noticeably distinct. This distinction vanishes for higher values of the velocity of the moving nanoparticle. Moreover, for a constant level of the moving nanoparticle velocity, an obvious distinction occurs for higher values of the slenderness ratio of the EQS as the scale effect becomes greater. For instantce, in the case of $V_N = 0.1$, the results of the NEB for $\mu = 0.3$ and 0.5 are up to 5 percent lower than those of the NHOB for $\lambda \geq 70$ and 85, correspondingly. It means that beyond the slenderness ratio of the EQS, the scale effect parameter could cause an

Table 2
Reliable ranges of the normalized velocity of the moving nanoparticle for successful capturing the DAFs of the NHOBT by the NEBT and NTBT according to the required accuracy.

	NEBT		NTBT	
	$e_{rel} \leq 5$percent[a]	$e_{rel} \leq 10$percent	$e_{rel} \leq 5$percent	$e_{rel} \leq 10$percent
$\lambda = 10$				
$\mu = 0.0$	–	–	–	–
$\mu = 0.3$	–	–	[0.2,0.3], [0.65,0.9]	[0.2,0.4], [0.65,1]
$\mu = 0.5$	–	–	[0.15,0.25]	[0.1,0.27], [0.55,0.65], [0.9,1]
$\lambda = 30$				
$\mu = 0.0$	[0,1]	[0,1]	[0,1]	[0,1]
$\mu = 0.3$	–	–	–	[0.35,0.8], [0.9,1]
$\mu = 0.5$	–	[0.95,1]	[0.41,0.48], [0.76,1]	[0.37,0.53], [0.65,1]
$\lambda = 50$				
$\mu = 0.0$	[0,1]	[0,1]	[0,1]	[0,1]
$\mu = 0.3$	–	–	[0.5,0.87]	[0,0.14], [0.27,1]
$\mu = 0.5$	–	[0.95,1]	[0.4,0.45], [0.53,0.7], [0.82,1]	[0.25,1]
$\lambda = 70$				
$\mu = 0.0$	[0,1]	[0,1]	[0,1]	[0,1]
$\mu = 0.3$	–	[0,0.35], [0.65,1]	[0,0.2], [0.35,1]	[0,0.27], [0.33,1]
$\mu = 0.5$	–	[0,0.25], [0.55,0.75], [0.85,1]	[0.3,0.43], [0.47,0.55], [0.6,0.65], [0.7,1]	[0,0.18], [0.3,1]
$\lambda = 90$				
$\mu = 0.0$	[0,1]	[0,1]	[0,1]	[0,1]
$\mu = 0.3$	[0,0.43]	[0,0.95]	[0,0.33], [0.45,1]	[0,1]
$\mu = 0.5$	[0,0.2]	[0,0.35], [0.42,1]	[0,0.2], [0.35,0.75], [0.9,1]	[0,0.27], [0.34,1]

[a] *Note:* The parameter e_{rel} stands for the relative error of the DAF of the NEBT or NTBT with respect to the DAF of the NHOBT.

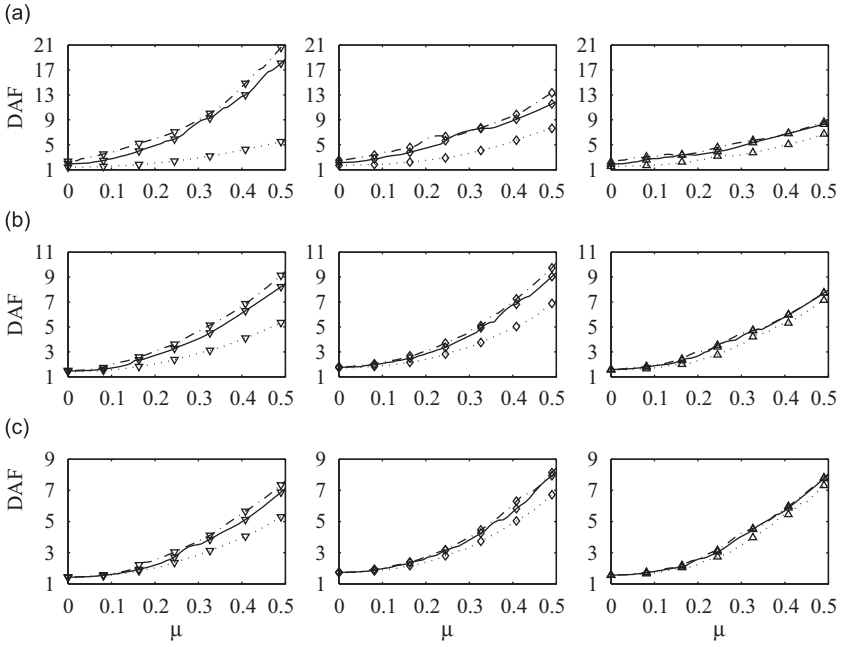

Fig. 5. Effect of the scale effect parameter on dynamic amplitude factor of the ECS for various values of moving nanoparticle velocity: (a) $\lambda = 10$, (b) $\lambda = 30$, (c) $\lambda = 50$; ((▽) $V_N = 0.3$, (◇) $V_N = 0.7$, (△) $V_N = 1.0$; (...) NEBT, (–.–) NTBT, (—) NHOBT).

increase in the difference between the results of the NEB with those of the NTB and NHOB. This is mainly due to the incorporation of the small scale effect into the shear strain energy of the nanotube structures modeled by the nonlocal shear deformable beam models. In other words, neither the shear stress nor the size effect parameter associated with the shear stress is included in the formulation of the nanotube structures using NEBT. In the case of $V_N = 0.1$, the predicted DAFs by the NTBT for $\mu = 0$, 0.3 and 0.5 demonstrate up to 5 percent higher than those of the NHOB for $\lambda \geq 20$, 70 and 85,

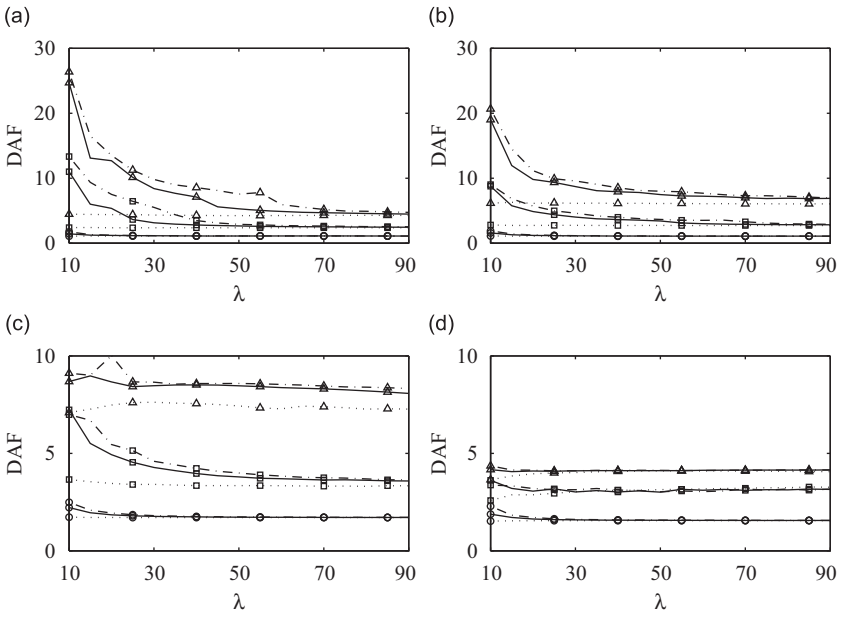

Fig. 6. Effect of the slenderness ratio of the ECS on the dynamic amplitude factor of the ECS for various values of moving nanoparticle velocity and scale effect parameter: (a) $V_N = 0.1$, (b) $V_N = 0.3$, (c) $V_N = 0.5$, (d) $V_N = 1.0$; ((◦) $\mu = 0.0$, (□) $\mu = 0.3$, (△) $\mu = 0.5$; (...) NEBT, (−.−) NTBT, (—) NHOBT).

correspondingly. Additionally, for high levels of the moving nanoparticle velocity ($V_N \geq 0.5$), the difference between the results of the NTB and those of the NHOB would generally lessen. For example, in the case of $V_N = 1$, the NTBT could reproduce the DAFs of the NHOB with relative error less than 5 percent for a nanotube structure with $\lambda \geq 20$ and $\mu \leq 0.5$.

6. Conclusions

Vibration of nanotube structures under a moving nanoparticle has been studied by utilizing the nonlocal continuum mechanics of Eringen. To this end, the nanotube structure is simulated as an equivalent continuum structure (ECS) under excitation of the point load of the mass weight of the nanoparticle based on the nonlocal Euler–Bernoulli, Timoshenko and higher order beam theories. The capabilities of various nonlocal beam theories in capturing the dynamic response of the ECS are then examined through various numerical examples. The role of the scale effect parameter, the slenderness ratio of the ECS and velocity of the moving nanoparticle on the time history associated with both phases of vibration and maximum dynamic deflection of various nonlocal beams are scrutinized in some detail. The major results obtained are as follows:

1. The midspan deflections of the NTB and NHOB with high scale effect parameter grow considerably just after the moving nanoparticle passes the midspan point. This fact demonstrates that the nonlocal shear deformable beams not only introduce shear effect in the formulations of the governing equations but also take into account additional data of the scale effect in the vibration analyses of the nanotube structures under a moving nanoparticle.
2. The occurrence of the maximum dynamic deflections generally shifts from the excitation phase to the free vibration phase as the moving nanoparticle velocity passes the critical velocity. This matter would be more visible as the scale effect parameter increases.
3. The difference between the predicted dynamic amplitude factors (DAFs) of various nonlocal beams using the local continuum theory (i.e., $\mu = 0$) for different values of velocity becomes negligible as the slenderness ratio of the ECS increases. However, this fact is followed with the lower rate for the nonlocal beams having the higher scale effect parameter.
4. A suitable nonlocal beam theory for the problem should be employed according to the slenderness ratio of the ECS, scale effect parameter and velocity of the moving nanoparticle. In the case of very stocky nanotube structures ($\lambda = 10$), the DAFs of the NEB are impressively distinct from those of the NTB and NHOB, especially for high values of the normalized scale effect parameter ($\mu \geq 0.3$) and low levels of the moving nanoparticle velocity ($V_N < 0.4$). Increasing of the amount of the scale effect parameter would intensify the difference between the predicted DAFs of the NTB and those of the NHOB, particularly for low values of the slenderness ($\lambda \leq 30$) and low levels of moving nanoparticle velocity ($V_N \leq 0.2$). In such conditions, it is strictly recommended that the NHOBT should be used instead of the NTBT for a more rational study of the dynamic response of the nanotube structures under excitation of a moving nanoparticle.

5. An increase in the scale effect parameter would commonly result in the increase of the predicted values of DAFs irrespective of the assumed nonlocal beam theory. Generally, in stocky nanotube structures, the variation of the scale effect parameter would result in more effect on the variation of the predicted values of DAFs compared with that in slender nanotube structures. Furthermore, beyond the slenderness ratio of the EQS, the scale effect parameter could cause an increase in the difference between the DAFs of the nonlocal classical beam and those of the nonlocal shear deformable beams. This is mainly due to the incorporation of the scale effect parameter into the shear strain energy of the nanotube structures simulated by the nonlocal shear deformable beam models.

The practicability of constructing nanocars in the molecular scale as well as molecular delivery and transportation of nanoparticles by the nanotube structures such as CNTs encouraged the authors to investigate the effects of a moving nanoparticle on the vibration of nanotube structures. Moreover, studying vibration of nanotube structures under several moving nanoparticles or even embedded nanotube structures in an elastic or viscoelastic medium under moving nanoparticles could be considered as important directions for the future works. Although the current research may have no immediate application, the obtained results of the presented mathematical models might help the researchers to be aware of the effects of a moving nanoparticle on the dynamic response of nanotube structures.

Appendix A

A.1. Mode shapes of the simply supported NEB

The dynamic deflection of the NEB is considered a wave with frequency ϖ as $\overline{w}^E(\xi,\tau)=\mathcal{W}^E(\xi)e^{i\varpi\tau}$. Substituting this expression into Eq. (10) gives

$$\mathcal{W}^E_{,\xi\xi\xi\xi}+a^2\,\mathcal{W}^E_{,\xi\xi}-b^2\mathcal{W}^E=0, \tag{83}$$

where

$$a^2=\frac{\varpi^2(\mu^2+1/\lambda^2)}{1-(\mu\varpi/\lambda)^2},\quad b^2=\frac{\varpi^2}{1-(\mu\varpi/\lambda)^2}. \tag{84}$$

Therefore, the general solution of Eq. (83) is obtained as

$$\mathcal{W}^E(\xi)=\begin{cases} C_1\cosh(r_1\xi)+C_2\sinh(r_1\xi)+C_3\cos(r_2\xi)+C_4\sin(r_2\xi) & \text{if } \varpi<\lambda/\mu,\\ C_1'\cosh(r_1'\xi)+C_2'\sinh(r_1'\xi)+C_3'\cosh(r_2'\xi)+C_4'\sinh(r_2'\xi) & \text{if } \varpi>\lambda/\mu,\end{cases} \tag{85}$$

where

$$r_1=\sqrt{\frac{-a^2+\sqrt{a^4+4b^2}}{2}},\quad r_2=\sqrt{\frac{a^2+\sqrt{a^4+4b^2}}{2}},$$

$$r_1'=\sqrt{\frac{a^2+\sqrt{a^4-4b^2}}{2}},\quad r_2'=\sqrt{\frac{a^2-\sqrt{a^4-4b^2}}{2}}. \tag{86}$$

Moreover, $\lambda/\mu=L_b^2/(e_0ar_b)$ implies a fairly high quantity especially for a slender beam. Thus, it is rationally assumed that the first dominant frequencies of the nanostructure would satisfy the condition $\varpi<\lambda/\mu$. Additionally, in the case of simply supported NEB (i.e., $\overline{w}^E(0,\tau)=\overline{w}^E(1,\tau)=0, M_b^E(0,\tau)=M_b^E(1,\tau)=0$); as a result, the following equations should be satisfied at both ends of the NEB (i.e., $\xi=0$ and 1):

$$\mathcal{W}^E=0,$$

$$\left(\left(\frac{\mu\varpi}{\lambda}\right)^2-1\right)\mathcal{W}^E_{,\xi\xi}-(\mu\varpi)^2\mathcal{W}^E=0, \tag{87}$$

or in a simpler form

$$\mathcal{W}^E(0)=\mathcal{W}^E(1)=0, \tag{88a}$$

$$\mathcal{W}^E_{,\xi\xi}(0)=\mathcal{W}^E_{,\xi\xi}(1)=0 \tag{88b}$$

Application of Eq. (88) into Eq. (85) for $\varpi<\lambda/\mu$ leads to

$$\begin{bmatrix} r_1^2 & 0 & -r_2^2 & 0\\ 1 & 0 & 1 & 0\\ \cosh(r_1) & \sinh(r_1) & \cos(r_2) & \sin(r_2)\\ r_1^2\cosh(r_1) & r_1^2\sinh(r_1) & -r_2^2\cos(r_2) & -r_2^2\sin(r_2)\end{bmatrix}\begin{Bmatrix} C_1\\ C_2\\ C_3\\ C_4\end{Bmatrix}=\begin{Bmatrix} 0\\ 0\\ 0\\ 0\end{Bmatrix}. \tag{89}$$

A solution to this homogeneous system of equations exists only if the determinant of the coefficient's matrix set equal to zero; hence, $\mathcal{W}^E(\xi)=C_4\sin(n\pi\xi)$ is derived as a nontrivial solution of Eq. (89); subsequently, $\phi_n^w(\xi)=\sin(n\pi\xi)$ is introduced as the n th mode shape of deflection for a simply supported NEB.

A.2. Mode shapes of the simply supported NTB

The mode solution for Eq. (25) could be assumed as

$$\overline{w}^{\mathrm{T}}(\xi,\tau)=\mathcal{W}^{\mathrm{T}}(\xi)\,\mathrm{e}^{\mathrm{i}\varpi\tau}, \tag{90a}$$

$$\overline{\theta}^{\mathrm{T}}(\xi,\tau)=\Theta^{\mathrm{T}}(\xi)\,\mathrm{e}^{\mathrm{i}\varpi\tau}. \tag{90b}$$

Substitution of Eq. (90) into Eq. (25) yields

$$(\mu^2\varpi^2-1)\,\mathcal{W}^{\mathrm{T}}_{,\xi\xi\xi}-\varpi^2\mathcal{W}^{\mathrm{T}}+\Theta^{\mathrm{T}}_{,\xi}=0, \tag{91a}$$

$$((1+\mu^2\varpi^2)/\lambda^2-\eta)\,\Theta^{\mathrm{T}}_{,\xi\xi}+\Theta^{\mathrm{T}}-\mathcal{W}^{\mathrm{T}}_{,\xi}=0. \tag{91b}$$

The parameter Θ^{T} could be omitted between Eqs. (91a) and (91b) such that

$$\mathcal{W}^{\mathrm{T}}_{,\xi\xi\xi\xi\xi}+a^2\,\mathcal{W}^{\mathrm{T}}_{,\xi\xi\xi}-b^2\,\mathcal{W}^{\mathrm{T}}=0, \tag{92}$$

where

$$a^2=\frac{(1+\mu^2\varpi^2)/\lambda^2-\eta-\mu^2}{(1/\varpi^2-\mu^2)((1+\mu^2\varpi^2)/\lambda^2-\eta)},$$

$$b^2=\frac{1}{(1/\varpi^2-\mu^2)(\eta-(1+\mu^2\varpi^2)/\lambda^2)}. \tag{93}$$

The general solution of Eq. (92) is

$$\mathcal{W}^{\mathrm{T}}(\xi)=\begin{cases}C_1\cosh(r_1\xi)+C_2\sinh(r_1\xi)+C_3\cos(r_2\xi)+C_4\sin(r_2\xi) & \text{if } \mu\varpi<1,\\ C_1'\cosh(r_1'\xi)+C_2'\sinh(r_1'\xi)+C_3'\cosh(r_2'\xi)+C_4'\sinh(r_2'\xi) & \text{if } \mu\varpi>\sqrt{\lambda^2(\eta+\mu^2)-1},\end{cases} \tag{94}$$

where

$$r_1=\sqrt{\frac{-a^2+\sqrt{a^4+4b^2}}{2}},\quad r_2=\sqrt{\frac{a^2+\sqrt{a^4+4b^2}}{2}},$$

$$r_1'=\sqrt{\frac{a^2+\sqrt{a^4-4b^2}}{2}},\quad r_2'=\sqrt{\frac{a^2-\sqrt{a^4-4b^2}}{2}}. \tag{95}$$

It is assumed that the condition $\mu\varpi<1$ would be satisfied especially for the lower modes of vibration. According to Eqs. (91a) and (94), the expression for $\Theta(\xi)$ is obtained as

$$\Theta^{\mathrm{T}}(\xi)=\frac{\kappa_1}{r_1}[C_1\sinh(r_1\xi)+C_2\cosh(r_1\xi)]+\frac{\kappa_2}{r_2}[C_3\sin(r_1\xi)-C_4\cos(r_1\xi)], \tag{96}$$

where $\kappa_1=\varpi^2+r_1^2(1-\mu^2\varpi^2)$ and $\kappa_2=\varpi^2-r_2^2(1-\mu^2\varpi^2)$. In the case of a simply supported NTB (i.e., $\overline{w}^{\mathrm{T}}(0,\tau)=\overline{w}^{\mathrm{T}}(1,\tau)=0, M_b^{\mathrm{T}}(0,\tau)=M_b^{\mathrm{T}}(1,\tau)=0$), the following conditions should be satisfied at both ends of the nanostructure (i.e., $\xi=0$ and 1)

$$\mathcal{W}^{\mathrm{T}}=0, \tag{97a}$$

$$(\varpi^2/\lambda^2-\eta)\Theta^{\mathrm{T}}_{,\xi}-\varpi^2\mathcal{W}^{\mathrm{T}}=0, \tag{97b}$$

Eq. (97) could be simplified to

$$\mathcal{W}^{\mathrm{T}}(0)=\mathcal{W}^{\mathrm{T}}(1)=0, \tag{98a}$$

$$\Theta^{\mathrm{T}}_{,\xi}(0)=\Theta^{\mathrm{T}}_{,\xi}(1)=0 \tag{98b}$$

Application of the conditions in Eq. (98) to Eqs. (94) and (96) leads to

$$\begin{bmatrix} 1 & 0 & 1 & 0 \\ \cosh(r_1) & \sinh(r_1) & \cos(r_2) & \sin(r_2) \\ \kappa_1 & 0 & \kappa_2 & 0 \\ \kappa_1\cosh(r_1) & \kappa_1\sinh(r_1) & \kappa_2\sin(r_2) & \kappa_2\cos(r_2) \end{bmatrix} \begin{Bmatrix} C_1 \\ C_2 \\ C_3 \\ C_4 \end{Bmatrix} = \begin{Bmatrix} 0 \\ 0 \\ 0 \\ 0 \end{Bmatrix}, \tag{99}$$

by setting the determinant of the coefficient's matrix equal to zero, a nontrivial solution of Eq. (99) is obtained as

$$\mathcal{W}^{\mathrm{T}}(\xi) = C_4 \sin(n\pi\xi),$$

$$\Theta^{\mathrm{T}}(\xi) = C_4 \frac{\kappa_2}{r_2} \cos(n\pi\xi). \tag{100}$$

As a result, $\phi_n^w(\xi) = \sin(n\pi\xi)$ and $\phi_n^\theta(\xi) = \cos(n\pi\xi)$ are introduced as the n th mode shapes of the deflection and rotation fields for the simply supported NTB.

A.3. Mode shapes of the simply supported NHOB

The mode solution for Eq. (47) is assumed as

$$\overline{w}^H(\xi,\tau) = \mathcal{W}^H(\xi)\mathrm{e}^{\mathrm{i}\varpi\tau}, \tag{101a}$$

$$\overline{\psi}^H(\xi,\tau) = \Psi^H(\xi)\mathrm{e}^{\mathrm{i}\varpi\tau}. \tag{101b}$$

Substitution of Eq. (101) into Eq. (47) yields

$$-\varpi^2\mathcal{W}^H+\mu^2\varpi^2W^H_{,\xi\xi}-\gamma_1^2\varpi^2(\Psi^H-\mu^2\Psi^H_{,\xi\xi})+\gamma_2^2\varpi^2(\mathcal{W}^H_{,\xi\xi}-\mu^2\mathcal{W}^H_{,\xi\xi\xi\xi})-\gamma_3^2(\Psi^H_{,\xi}+\mathcal{W}^H_{,\xi\xi})-\gamma_4^2\Psi^H_{,\xi\xi\xi}+\mathcal{W}^H_{,\xi\xi\xi\xi}=0,$$

$$-\varpi^2\Psi^H+\mu^2\varpi^2\Psi^H_{,\xi\xi}+\gamma_6^2\varpi^2(\mathcal{W}^H_{,\xi}-\mu^2\mathcal{W}^H_{,\xi\xi\xi})+\gamma_7^2(\Psi^H+\mathcal{W}^H_{,\xi})-\gamma_8^2\Psi^H_{,\xi\xi}+\gamma_9^2\mathcal{W}^H_{,\xi\xi\xi}=0. \tag{102}$$

We define the operator $D=\square_{,\xi}$; therefore

$$\begin{bmatrix} (1-\mu^2\varpi^2\gamma_2^2)D^4+(\mu^2\varpi^2+\gamma_2^2\varpi^2-\gamma_3^2)D^2-\varpi^2 & -\gamma_4^2D^3+\gamma_1^2\mu^2\varpi^2D^2-\gamma_3^2D-\gamma_1^2\varpi^2 \\ (\gamma_9^2-\mu^2\varpi^2\gamma_6^2)D^3+(\gamma_7^2+\gamma_6^2\varpi^2)D & (-\gamma_8^2+\mu^2\varpi^2)D^2+(\gamma_7^2-\varpi^2) \end{bmatrix} \times \begin{Bmatrix} \mathcal{W}^H(\xi) \\ \Psi^H(\xi \end{Bmatrix} = \begin{Bmatrix} 0 \\ 0 \end{Bmatrix}. \tag{103}$$

A solution for $\mathcal{W}^H(\xi)$ in Eq. (103) is sought of the form $\mathrm{e}^{r\xi}$, which when substituted into Eq. (103) leads to

$$a_6\,r^6+a_5\,r^5+a_4\,r^4+a_3\,r^3+a_2\,r^2+a_1\,r+a_0=0, \tag{104}$$

where

$$a_6=\gamma_4^2\gamma_9^2-\gamma_8^2+\mu^2\varpi^2(\gamma_2^2\gamma_8^2+1-\mu^2\varpi^2\gamma_2^2-\gamma_4^2\gamma_6^2),$$

$$a_5=-\mu^2\varpi^2\gamma_1^2(\gamma_9^2-\mu^2\varpi^2\gamma_6^2),$$

$$a_4=(\gamma_7^2-\varpi^2)(1-\mu^2\varpi^2\gamma_2^2)+\gamma_4^2(\gamma_7^2+\varpi^2\gamma_6^2)+\gamma_3^2(\gamma_9^2-\mu^2\varpi^2\gamma_6^2)+\varpi^2(\mu^2+\gamma_2^2)-\gamma_3^2,$$

$$a_3=\varpi^2\gamma_1^2(\gamma_9^2-\mu^2\gamma_7^2-2\mu^2\varpi^2\gamma_6^2),$$

$$a_2=\varpi^2(\mu^2+\gamma_2^2)+\varpi^2\gamma_3^2(1+\gamma_6^2),$$

$$a_1=\gamma_1^2\varpi^2(\gamma_7^2+\varpi^2\gamma_6^2),$$

$$a_0=-\varpi^2(\gamma_7^2-\varpi^2). \tag{105}$$

Therefore, the general solution for Eq. (103) is written as follows:

$$\mathcal{W}^H(\xi)=\sum_{I=1}^{6}C_I'\,\mathrm{e}^{r_I\xi}, \tag{106a}$$

$$\Psi^H(\xi)=\sum_{I=1}^{6}C_I'\varrho_I\,\mathrm{e}^{r_I\xi}, \tag{106b}$$

where

$$\varrho_I=-\frac{(\gamma_9^2-\mu^2\varpi^2\gamma_6^2)\,r_I^3+(\gamma_7^2+\gamma_6^2\varpi^2)r_I}{(\gamma_7^2-\varpi^2)+r_I^2\,(\mu^2\varpi^2-\gamma_8^2)}. \tag{107}$$

It can be shown numerically that Eq. (104) have four real and two complex roots of the form $\pm\alpha_1, \pm\alpha_2, \alpha_3 \pm i\beta_3$ in most of the cases. Hence, the appropriate mode shapes of the NHOB are obtained as

$$\mathcal{W}^H(\xi) = C_1\cosh(\alpha_1\xi)+C_2\sinh(\alpha_1\xi)+C_3\cosh(\alpha_2\xi)+C_4\sinh(\alpha_2\xi)+C_5 e^{\alpha_3\xi}\cos(\beta_3\xi)+C_6 e^{\alpha_3\xi}\sin(\beta_3\xi),$$

$$\begin{aligned}\Psi^H(\xi) = {} & C_1\varrho_1\sinh(\alpha_1\xi)+C_2\varrho_1\cosh(\alpha_1\xi)+C_3\varrho_2\sinh(\alpha_2\xi)+C_4\varrho_2\cosh(\alpha_2\xi)+C_5 e^{\alpha_3\xi}(\mathcal{A}\cos(\beta_3\xi)-\mathcal{B}\sin(\beta_3\xi))\\ & +C_6 e^{\alpha_3\xi}(\mathcal{B}\cos(\beta_3\xi)+\mathcal{A}\sin(\beta_3\xi)),\end{aligned} \tag{108}$$

where

$$\varrho_I = \varrho_I(r_I=\alpha_I), \quad I=1,2,$$

$$\mathcal{A} = \frac{\alpha_3((T+\alpha_3^2S)(P+\alpha_3^2Q)+\beta_3^2(TQ-3SP+2\alpha_3^2SQ)+\beta_3^4SQ)}{\alpha_3^4Q^2+(P-\beta_3^2Q)^2+2\alpha_3^2Q(P+\beta_3^2Q)},$$

$$\mathcal{B} = \frac{\beta_3(\alpha_3^2SQ+(T-\beta_3^2S)(P-\beta_3^2Q)+\alpha_3^2(3SP-TQ+2\beta_3^2SQ))}{\alpha_3^4Q^2+(P-\beta_3^2Q)^2+2\alpha_3^2Q(P+\beta_3^2Q)}, \tag{109}$$

in which

$$S=\mu^2\varpi^2\gamma_6^2-\gamma_9^2, \quad T=-(\gamma_7^2+\gamma_6^2\varpi^2), \quad P=\gamma_7^2-\varpi^2, \quad Q=\mu^2\varpi^2-\gamma_8^2 \tag{110}$$

In the case of simply supported boundary conditions [41]

$$\overline{w}^H(0,\tau)=\overline{w}^H(1,\tau)=0, \tag{111a}$$

$$M_b^H(0,\tau)=M_b^H(1,\tau)=0, \tag{111b}$$

$$P_b^H(0,\tau)=P_b^H(1,\tau)=0, \tag{111c}$$

therefore

$$\mathcal{W}^H(0)=\mathcal{W}^H(1)=0, \tag{112a}$$

$$\mathcal{W}^H_{,\xi\xi}(0)=\mathcal{W}^H_{,\xi\xi}(1)=0, \tag{112b}$$

$$\Psi^H_{,\xi}(0)=\Psi^H_{,\xi}(1)=0. \tag{112c}$$

The conditions in Eq. (111) are enforced to Eq. (108):

$$\mathbf{KC}=\mathbf{0}, \tag{113}$$

where

$$\mathbf{C}=\{C_1,C_2,C_3,C_4,C_5,C_6\}^{\mathrm{T}},$$

$$K_{11}=1, \quad K_{12}=1, \quad K_{15}=1, \quad K_{21}=\cosh(\alpha_1), \quad K_{22}=\sinh\alpha_1, \quad K_{23}=\cosh(\alpha_2), \quad K_{24}=\sinh(\alpha_2),$$

$$K_{25}=e^{\alpha_3}\cos(\beta_3), \quad K_{26}=e^{\alpha_3}\sin(\beta_3), \quad K_{31}=\alpha_1^2, \quad K_{33}=\alpha_2^2, \quad K_{35}=\alpha_3^2-\beta_3^2, \quad K_{36}=2\alpha_3\beta_3,$$

$$K_{41}=\alpha_1^2\cosh(\alpha_1), \quad K_{42}=\alpha_1^2\sinh(\alpha_1), \quad K_{43}=\alpha_2^2\cosh(\alpha_2), \quad K_{44}=\alpha_2^2\sinh(\alpha_2),$$

$$K_{45}=e^{\alpha_3}[\alpha_3^2\cos(\beta_3)-\beta_3^2\cos(\beta_3)-2\alpha_3\beta_3\sin(\beta_3)], \quad K_{46}=e^{\alpha_3}[\alpha_3^2\sin(\beta_3)-\beta_3^2\sin(\beta_3)+2\alpha_3\beta_3\cos(\beta_3)],$$

$$K_{51}=\varrho_1\alpha_1, \quad K_{53}=\varrho_2\alpha_2, \quad K_{55}=\alpha_3\mathcal{A}-\beta_3\mathcal{B}, \quad K_{56}=\beta_3\mathcal{A}+\alpha_3\mathcal{B},$$

$$K_{61}=\varrho_1\alpha_1\cosh(\alpha_1), \quad K_{62}=\varrho_1\alpha_1\sinh(\alpha_1), \quad K_{63}=\varrho_2\alpha_2\cosh(\alpha_2), \quad K_{64}=\varrho_2\alpha_2\sinh(\alpha_2),$$

$$K_{65}=e^{\alpha_3}[(\alpha_3\mathcal{A}-\beta_3\mathcal{B})\cos(\beta_3)-(\alpha_3\mathcal{B}+\beta_3\mathcal{A})\sin(\beta_3)],$$

$$K_{66}=e^{\alpha_3}[(\alpha_3\mathcal{A}-\beta_3\mathcal{B})\sin(\beta_3)+(\beta_3\mathcal{A}+\alpha_3\mathcal{B})\cos(\beta_3)]. \tag{114}$$

The other not mentioned elements of **K** are equal to zero. The determinant of **K** is set equal to zero to obtain nontrivial solution:

$$\mathcal{W}^H(\xi)=C_6\sin(n\pi\xi), \quad \Psi^H(\xi)=C_6\mathcal{B}\cos(n\pi\xi). \tag{115}$$

Therefore, $\phi_n^w(\xi)=\sin(n\pi\xi)$ and $\phi_n^\psi(\xi)=\cos(n\pi\xi)$ are considered as the corresponding mode shapes of the deflection and rotation fields for the simply supported NHOB.

References

[1] G. Hummer, J.C. Rasaiah, J.P. Noworyta, Water conduction through the hydrophobic channel of a carbon nanotube, *Nature* 414 (2001) 188–190.
[2] B.C. Regan, S. Aloni, R.O. Ritchie, U. Dahmen, A. Zettl, Carbon nanotubes as nanoscale mass conveyors, *Nature* 428 (2004) 924–927.
[3] M. Majumder, N. Chopra, R. Andrews, B.J. Hinds, Nanoscale hydrodynamics: enhanced flow in carbon nanotubes, *Nature* 438 (2005) 44.
[4] P.A.E. Schoen, J.H. Walther, S. Arcidiacono, D. Poulikakos, P. Koumoutsakos, Nanoparticle traffic on helical tracks: thermophoretic mass transport through carbon nanotubes, *Nano Letters* 6 (9) (2006) 1910–1917.
[5] S.P. Fletcher, F. Dumur, M.M. Pollard, B.L. Feringa, A reversible, unidirectional molecular rotary motor driven by chemical energy, *Science* 310 (2006) 80–82.
[6] D. Pijper, R.A. van Delden, A. Meetsma, B.L. Feringa, Acceleration of a nanomotor: electronic control of the rotary speed of a light-driven molecular rotor, *Journal of the American Chemical Society* 127 (2005) 17612–17613.
[7] Y. Shirai, A.J. Osgood, Y. Zhao, K.F. Kelly, J.M. Tour, Directional control in thermally driven single-molecule nanocars, *Nano Letters* (2005) 2330–2334.
[8] Y. Shirai, A.J. Osgood, Y. Zhao, Y. Yao, L. Saudan, H. Yang, C. Yu-Hung, L.B. Alemany, T. Sasaki, J.F. Morin, J. Guerrero, K.F. Kelly, J.M. Tour, Surface-rolling molecules, *Journal of the American Chemical Society* 128 (2006) 4854–4864.
[9] Y. Shirai, J.F. Morin, T. Sasaki, J. Guerrero, J.M. Tour, Recent progress on nanovehicles, *Chemical Society Reviews* 35 (2006) 1043–1055.
[10] R.A. Van Delden, N. Koumura, A. Schoevaars, A. Meetsma, B.L. Feringa, A donor-acceptor substituted molecular motor: unidirectional rotation driven by visible light, *Organic and Biomolecular Chemistry* 1 (2003) 33–35.
[11] R.A. Van Delden, M.K.J. Ter Wiel, M.M. Pollard, J. Vicario, N. Koumura, B.L. Feringa, Unidirectional molecular motor on a gold surface, *Nature* 437 (2005) 1337–1340.
[12] F. Chiaravalloti, L. Gross, K.H. Rieder, S. Stojkovic, A. Gourdon, C. Joachim, F. Moresco, A rack-and-pinion device at the molecular scale, *Nature Materials* 6 (2007) 30–33.
[13] L. Gross, K.H. Rieder, F. Moresco, S. Stojkovic, A. Gourdon, C. Joachim, Trapping and moving single metal atoms with a 6-leg molecule, *Nature Materials* 4 (12) (2005) 892–895.
[14] S.S. Gupta, R.C. Batra, Continuum structures equivalent in normal mode vibrations to single-walled carbon nanotubes, *Computational Materials Science* 43 (2008) 715–723.
[15] R.C. Picu, A non-local formulation of rubber elasticity, *Journal of Multiscale Computational Engineering* 1 (2003) 23–32.
[16] J. Peddieson, G.R. Buchanan, R.P. McNitt, Application of nonlocal continuum models to nanotechnology, *International Journal of Engineering Science* 41 (2003) 305–312.
[17] Q. Wang, K.M. Liew, Application of nonlocal continuum mechanics to static analysis of micro- and nano-structures, *Physics Letters A* (2007) 236–242.
[18] L.J. Sudak, Column buckling of multiwalled carbon nanotubes using nonlocal continuum mechanics, *Journal of Applied Physics* 94 (2003) 7281–7287.
[19] T. Murmu, S.C. Pradhan, Buckling analysis of a single-walled carbon nanotube embedded in an elastic medium based on nonlocal elasticity and Timoshenko beam theory and using DQM, *Physica E: Low-dimensional Systems and Nanostructures* 41 (2009) 1232–1239.
[20] Q. Wang, V.K. Varadan, S.T. Quek, Small scale effect on elastic buckling of carbon nanotubes with nonlocal continuum models, *Physics Letters A* 357 (2006) 130–135.
[21] S. Adali, Variational principles for multi-walled carbon nanotubes undergoing buckling based on nonlocal elasticity theory, *Physics Letters A* 372 (2008) 5701–5705.
[22] G.D. Mahan, Oscillations of a thin hollow cylinder: carbon nanotubes, *Physical Review B* 65 (2002) 235402.
[23] J. Yoon, C.Q. Ru, A. Mioduchowski, Noncoaxial resonance of an isolated multiwall carbon nanotube, *Physical Review B* 66 (2002) 233402.
[24] T. Murmu, S.C. Pradhan, Small-scale effect on the vibration of nonuniform nanocantilever based on nonlocal elasticity theory, *Physica E: Low-dimensional Systems and Nanostructures* 41 (2009) 1451–1456.
[25] I.A. Guz, J.J. Rushchitsky, Computational simulation of harmonic wave propagation in fibrous micro- and nanocomposites, *Composites Science and Technology* 67 (2007) 861–866.
[26] H. Heirechea, A. Tounsi, A. Benzair, M. Maachoua, E.A. Adda Bedia, Sound wave propagation in single-walled carbon nanotubes using nonlocal elasticity, *Physica E* 40 (2008) 2791–2799.
[27] Y.G. Hu, K.M. Liew, Q. Wang, X.Q. He, B.I. Yakobson, Nonlocal shell model for elastic wave propagation in single- and double-walled carbon nanotubes, *Journal of the Mechanics and Physics of Solids* 56 (2008) 3475–3485.
[28] L. Wang, Vibration and instability analysis of tubular nano- and micro-beams conveying fluid using nonlocal elastic theory, *Physica E: Low-dimensional Systems and Nanostructures*, 41 (2009) 1835–1840.
[29] L. Wang, Dynamical behaviors of double-walled carbon nanotubes conveying fluid accounting for the role of small length scale, *Computational Materials Science* 45 (2009) 584–588.
[30] H.-L. Lee, W.-J. Chang, Vibration analysis of a viscous-fluid-conveying single-walled carbon nanotube embedded in an elastic medium, *Physica E: Low-dimensional Systems and Nanostructures* 41 (2009) 529–532.
[31] J.N. Reddy, Nonlocal theories for bending, buckling and vibration of beams, *International Journal of Engineering Science* 45 (2007) 288–307.
[32] M. Aydogdu, A general nonlocal beam theory, buckling and vibration: its application to nanobeam bending, *Physica E: Low-dimensional Systems and Nanostructures* 41 (2009) 1651–1655.
[33] A.C. Eringen, Nonlocal polar elastic continua, *International Journal of Engineering Science* 10 (1972) 1–16.
[34] A.C. Eringen, On differential equations of nonlocal elasticity and solutions of screw dislocation and surface waves, *Journal of Applied Physics* 54 (1983) 4703–4710.
[35] A.C. Eringen, *Nonlocal Continuum Field Theories*, Springer, New York, 2002.
[36] L. Wang, H. Hu, Flexural wave propagation in single-walled carbon nanotubes, *Physical Review B* 71 (2005) 195412.
[37] Q. Wang, Q.K. Han, B.C. Wen, Estimate of material property of carbon nanotubes via nonlocal elasticity, *Advances in Theoretical and Applied Mechanics* 1 (2008) 1–10.
[38] Q. Wang, C.M. Wang, The constitutive relation and small scale parameter of nonlocal continuum mechanics for modelling carbon nanotubes, *Nanotechnology* 18 (2007) 075702.
[39] L. Frýba, *Vibration of Solids and Structures under Moving Loads*, Thomas Telford, London, 1999.
[40] S. Timoshenko, *Vibration Problems in Engineering*, third ed., Van Nostrand, Princeton, NJ, 1955.
[41] J.N. Reddy, *Mechanics of Laminated Composite Plates*, CRC Press, Boca Raton, FL, 1997.
[42] K. Kiani, A. Nikkhoo, B. Mehri, Prediction capabilities of classical and shear deformable beam models excited by a moving mass, *Journal of Sound and Vibration* 320 (2009) 632–648.
[43] H. Zhang, S.Y. Zhang, T.H. Wang, Flexural vibration analyses of piezoelectric ceramic tubes with mass loads in ultrasonic actuators, *Ultrasonics* 47 (2007) 82–89.